Energy consumption monitoring of the welding cells

Bc. Martin Roučka

Univerzita Tomáše Bati ve Zlíně

Fakulta aplikované informatiky

akademický rok: 2016/2017

ZADÁNÍ DIPLOMOVÉ PRÁCE

(PROJEKTU, UMĚLECKÉHO DÍLA, UMĚLECKÉHO VÝKONU)

Jméno a příjmení: **Bc. Martin Roučka**

Osobní číslo: **A15623**

Studijní program: **N3902 Inženýrská informatika**

Studijní obor: **Automatické řízení a informatika**

Forma studia: **prezenční**

Téma práce: **Monitorování spotřeby energie svařovacích buněk**

Téma anglicky: **Energy Consumption Monitoring of the Welding Cells**

Zásady pro vypracování:

1. Zpracujte literární rešerši na téma měření energií.

2. Vyberte vhodné typy měřicích přístrojů na základě požadavků dané aplikace.

3. Navrhněte způsob začlenění měřicího systému do svařovací buňky.

4. Realizujte systém měření, včetně podpůrného programového vybavení.

5. Proveďte praktické ověření funkce zařízení.

Rozsah diplomové práce:

Rozsah příloh:

Forma zpracování diplomové práce: **tištěná/elektronická**

Seznam odborné literatury:

1. **Automating with SIMATIC: Hardware and Software, Configuration and Programming, Data Communication, Operator Control and Monitoring, Hans Berger, 2016, ISBN: 978-3-89578-459-0.**

2. **Automating with SIMATIC S7-1500: Configuring, Programming and Testing with STEP 7 professional, Hans Berger, 2014, ISBN: 978-3-89578-404-0**

3. **Electrical and Electronics Measurements and Instrumentation: Prithwiraj Purkait, Budhaditya Biswas, Santanu Das, Chiranjib Koley, 2013, ISBN: 9789383286799**

4. **Technické prostředky Integrované automatizace, František Hruška, 2012, ISBN: 978 80 7454 234 3**

5. **Měření průtoku a výšky hladiny, Stanislav Ďaďo, Ludvík Bejček, Antonín Platil, 2005, ISBN: 80-7300-156-X.**

Vedoucí diplomové práce: **Ing. Petr Dostálek, Ph.D.**
                               Ústav automatizace a řídicí techniky

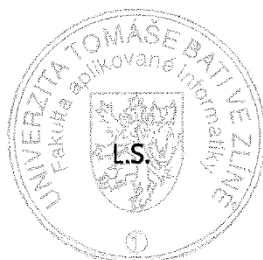Datum zadání diplomové práce: **3. března 2017**

Termín odevzdání diplomové práce: **22. května 2017**

Ve Zlíně dne 3. března 2017

doc. Mgr. Milan Adámek, Ph.D.   prof. Ing. Vladimír Vašek, CSc.
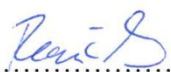*děkan*   *ředitel ústavu*

Prohlašuji, že

- beru na vědomí, že odevzdáním diplomové/bakalářské práce souhlasím se zveřejněním své práce podle zákona č. 111/1998 Sb. o vysokých školách a o změně a doplnění dalších zákonů (zákon o vysokých školách), ve znění pozdějších právních předpisů, bez ohledu na výsledek obhajoby;
- beru na vědomí, že diplomová/bakalářská práce bude uložena v elektronické podobě v univerzitním informačním systému dostupná k prezenčnímu nahlédnutí, že jeden výtisk diplomové/bakalářské práce bude uložen v příruční knihovně Fakulty aplikované informatiky Univerzity Tomáše Bati ve Zlíně a jeden výtisk bude uložen u vedoucího práce;
- byl/a jsem seznámen/a s tím, že na moji diplomovou/bakalářskou práci se plně vztahuje zákon č. 121/2000 Sb. o právu autorském, o právech souvisejících s právem autorským a o změně některých zákonů (autorský zákon) ve znění pozdějších právních předpisů, zejm. § 35 odst. 3;
- beru na vědomí, že podle § 60 odst. 1 autorského zákona má UTB ve Zlíně právo na uzavření licenční smlouvy o užití školního díla v rozsahu § 12 odst. 4 autorského zákona;
- beru na vědomí, že podle § 60 odst. 2 a 3 autorského zákona mohu užít své dílo – diplomovou/bakalářskou práci nebo poskytnout licenci k jejímu využití jen připouští-li tak licenční smlouva uzavřená mezi mnou a Univerzitou Tomáše Bati ve Zlíně s tím, že vyrovnání případného přiměřeného příspěvku na úhradu nákladů, které byly Univerzitou Tomáše Bati ve Zlíně na vytvoření díla vynaloženy (až do jejich skutečné výše) bude rovněž předmětem této licenční smlouvy;
- beru na vědomí, že pokud bylo k vypracování diplomové/bakalářské práce využito softwaru poskytnutého Univerzitou Tomáše Bati ve Zlíně nebo jinými subjekty pouze ke studijním a výzkumným účelům (tedy pouze k nekomerčnímu využití), nelze výsledky diplomové/bakalářské práce využít ke komerčním účelům;
- beru na vědomí, že pokud je výstupem diplomové/bakalářské práce jakýkoliv softwarový produkt, považují se za součást práce rovněž i zdrojové kódy, popř. soubory, ze kterých se projekt skládá. Neodevzdání této součásti může být důvodem k neobhájení práce.

Prohlašuji,

- že jsem na diplomové/bakalářské práci pracoval samostatně a použitou literaturu jsem citoval. V případě publikace výsledků budu uveden jako spoluautor.
- že odevzdaná verze diplomové práce a verze elektronická nahraná do IS/STAG jsou totožné.

Ve Zlíně, dne 19. 5. 2017

....
podpis diplomanta

ABSTRAKT

Cílem této diplomové práce je navrhnout systém, který bude schopen monitorovat celkovou spotřebu energie automatizovaných cel/buněk se svářecími roboty (zahrnuje elektrickou a pneumatickou energii). Výsledkem práce bude návrh měření spotřeby energie a následné zpracování, ukládání a vyhodnocování získaných informací s ohledem na náklady spojené se samotným monitorovacím systémem.

Klíčová slova:

Činný výkon, jalový výkon, zdánlivý výkon, elektroměr, průtokoměr, svářecí buňka, průtok stlačeného vzduchu, elektrická energie, spotřeba energie, funkční blok a datový blok.

ABSTRACT

This thesis is focused on the design of a system, which will be able to monitor total energy consumption of automatized cells with welding robots (it includes electrical and pneumatic energy). The purpose of this thesis is to design a measurement system of energy consumption; it follows processing, storing and evaluation of gained information with respect to costs associated with the monitoring system.

Keywords:

Active power, reactive power, apparent power, energy meter, flow meter, welding cell, compressed air flow, electric energy, energy consumption, function block and data block.

ACKNOWLEDGEMENTS

Acknowledgements, motto and a declaration of honor saying that the print version of the Bachelor's/Master's thesis and the electronic version of the thesis deposited in the IS/STAG system are identical, worded as follows:

I hereby declare that the print version of my Bachelor's/Master's thesis and the electronic version of my thesis deposited in the IS/STAG system are identical.

CONTENTS

INTRODUCTION

In past years, energy consumption was a highly discussed topic. World institutes, organizations, and committees are trying by their norms and standards to contribute to world energy consumption reduction. It has become a "hot" topic for several reasons. One of them, and probably the most important, is the ecological factor because energy production (heat energy and electric energy) is predominantly still done by burning fossil fuels. Potential annual savings of electric energy at an electric drive based on some German sources is approximately 27 billion kWh due to a balanced electric grid. It should be mentioned that electric drives are the predominant consumers of electric energy in the world (their consumption is up to 55% of electric energy in industry). Another reason to consider is the prediction of the ever-rising need for electric energy which raises its consumption. A world statistic shows that the highest demand for electricity is from Asian countries mainly, from China and India. Because of these reasons and many others, an energy management system could be established based on norms and standards which should contribute to saving energy and its cost by modern, computer-aided technologies. These computer-aided technologies can measure, control and optimize an industry process, as in this case, automated welding.

In this thesis will be described and designed an energy measurement system for welding cells of AWL-Techniek Company. A designed system should be integrated into all newly produced machines, and this add-on should be attractive by its functionalities and price for AWL customers.

I. THEORY

1 POWER OF ALTERNATING ELECTRIC CURRENT

This thesis is strictly focused on ordinary used electrical devices, which are powered from the electric grid (by alternating electric current). Electric energy may be taken from the electric grid through one phase or three phase (in the system of three wires or four wires), symmetrically or asymmetrically with sinusoidal or non-sinusoidal currents. Methods of electric energy consumption greatly vary and it is characterized by time course of the actual values of electric power $p(t)$.

1.1 Electric power of sinusoidal current

Electric power is a physical quantity, which describes performed electrical work per unit of time and it is described as the vector product of current and voltage.

$$p(t) = u(t)i(t) \tag{1}$$

Both current and voltage are dependent on time but their waveforms are generally periodic, most often with a sine wave.

$$u(t) = \sqrt{2}U sin(\omega t + \alpha) \tag{2}$$

$$i(t) = \sqrt{2}I sin(\omega t + \beta) \tag{3}$$

The expression: $\sqrt{2}U$ respective $\sqrt{2}I$ describes the maximum value of the AC voltage respective AC. Then we can substitute equations (2), (3) into the equation (1) and simplify it.

$$p(t) = \sqrt{2}U sin(\omega t + \alpha)\sqrt{2}I sin(\omega t + \beta) \tag{4}$$

$$p(t) = UI cos(\alpha - \beta) - UI cos(2\omega t + \alpha + \beta) \tag{5}$$

1.1.1 Active, reactive, apparent powers

In the case of alternating current, power is divided into following powers: active power, reactive power, apparent power. Apparent power is described as the absolute value of vector sum active and reactive power or product of RMS (Root Mean Square) voltage and current values:

$$|A| = \hat{U}\hat{I} = \sqrt{P^2 + Q^2} \tag{6}$$

Where P is active power and Q is reactive power. Unit of apparent power is $Volt-Amperes\ [VA]$. [1]

Average value of consumed/absorbed power (energy flow in one direction from the source to the load) is called active power which is calculated in this case by integrating of electrical work:

$$P = \frac{1}{T}\int_0^T p(t)dt = UIcos(\alpha - \beta) = UIcos\varphi \tag{7}$$

Expression $(\alpha - \beta)$ is known as power factor φ and it represents phase shift between the phase angle of the voltage (α) and phase angle of the current (β). The size of the phase shift depends on capacitance and inductance of the system. If $\varphi = 0$ then the system is purely resistive and behave as DC system $(\cos 0 = 1)$. Unit of active power is Watt $[W]$. [1]

As was previously mentioned, in electro-technics is used term reactive power. This power is absorbed/returned from/to the source in each cycle (caused by the capacitive or inductive load). It is represented as the imaginary axis of the vector diagram. Reactive power is then represented by the following equation.

$$Q = Asin(\alpha - \beta) = Asin\varphi \tag{8}$$

The units of reactive power are Volt-Amperes reactive (VAr). For an illustration of these powers are commonly used phasor represented by figure 1.
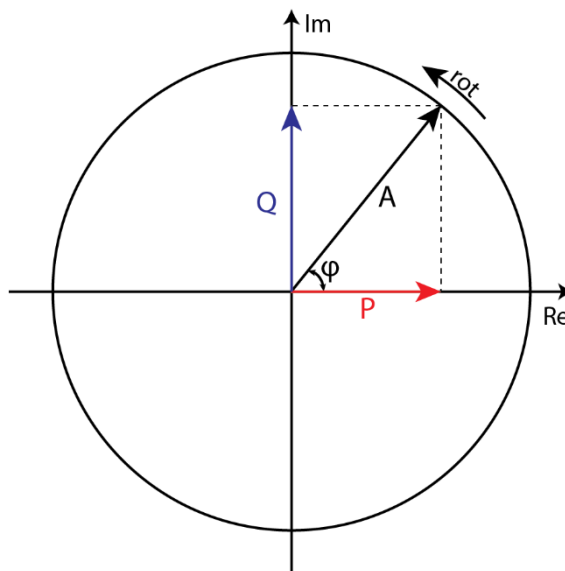
Figure 1: Phase diagram representing active, reactive and complex powers.

From phase diagram is obvious that $A = \sqrt{P^2 + Q^2}$, which describes the magnitude of apparent power.
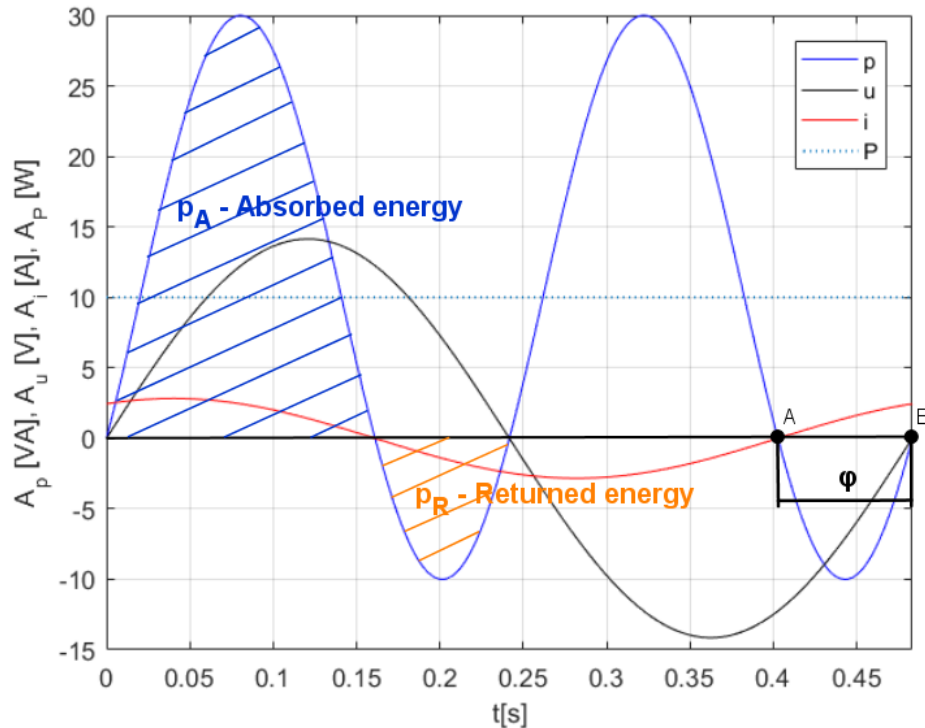
Figure 2: The waveforms of voltage, current and powers

Figure 2 describes waveforms of voltage, current and phase shift $\varphi = \frac{\pi}{3}$ between them (represented by points A, B). The figure describes also waveform of power in time, where power absorbed by the appliance is p_A and is power returned to the source from the appliance is p_R. The active/average power is here described as the vector, but as was written before active power is constant (here $P = 10W$). It is described as the line, due to better clarity. [1]

1.2 Electric power of non-sinusoidal current

In practice, waveforms are rarely sinusoidal. In fact, they are deformed by noise or any nonlinearity which also affects the value of active power, thus the calculation of active, reactive and apparent power will be different than in the case of sinusoidal current.

1.2.1 Active power calculation in case of non-sinusoidal current

To analyze and describe nonlinear waveform mathematically is better to use discrete mathematics. The fact is that most of the today's digital measuring devices are working

only with it and non-sinusoidal waveforms are easier to describe (in the case of continuous math the waveform could be composed of series of cos and sin functions where each sin/cos function represents one harmonics). To convert a continuous waveform into a discrete one is necessary to sample the waveform and register value of each sample in time. Then the equation (1) can be rewritten to the numerical form:

$$p_k(t_k) = i_k(t_k)u_k(t_k)\cos\varphi_k(t_k) \tag{9}$$

Where p_k represents apparent power value in the time sample k, the sampling of power is represented in the following figure:
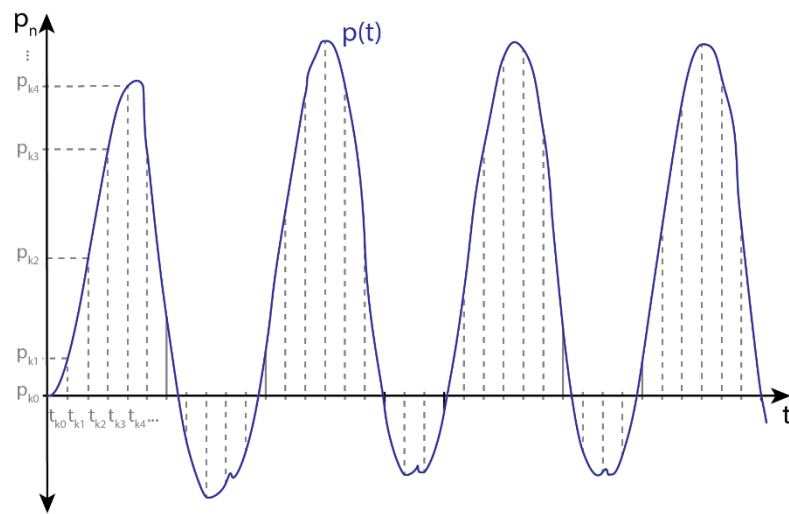
Figure 3: Sampling of the non-sinusoidal waveform, power sampling.

With rising number of samples n is also rising the accuracy of the numerical method which replaces continuous representation. From recorded values of current and voltage can be calculated and visualized the flow of the power (figure 3) thus can be calculated average power, where integral is replaced by sum and period time by the total number of samples.

$$P = \frac{1}{n}\sum_{k=0}^{n} i_k u_k \cos\varphi_k = \frac{1}{n}\left[i_0 u_0 \cos\varphi_0 + \sum_{k=1}^{n} i_k u_k \cos\varphi_k\right] \tag{10}$$

Waveforms of non-sinusoidal current, voltage, apparent power and active power are shown in the following figure. For calculations of power in this subchapter is used a different frequency, because of a better illustration of differences in peak values. These nonlinear waveforms are obtained by measurement on a non-linear transformer, which also caused a voltage drop. It naturally affects active power which value is changed. [1]
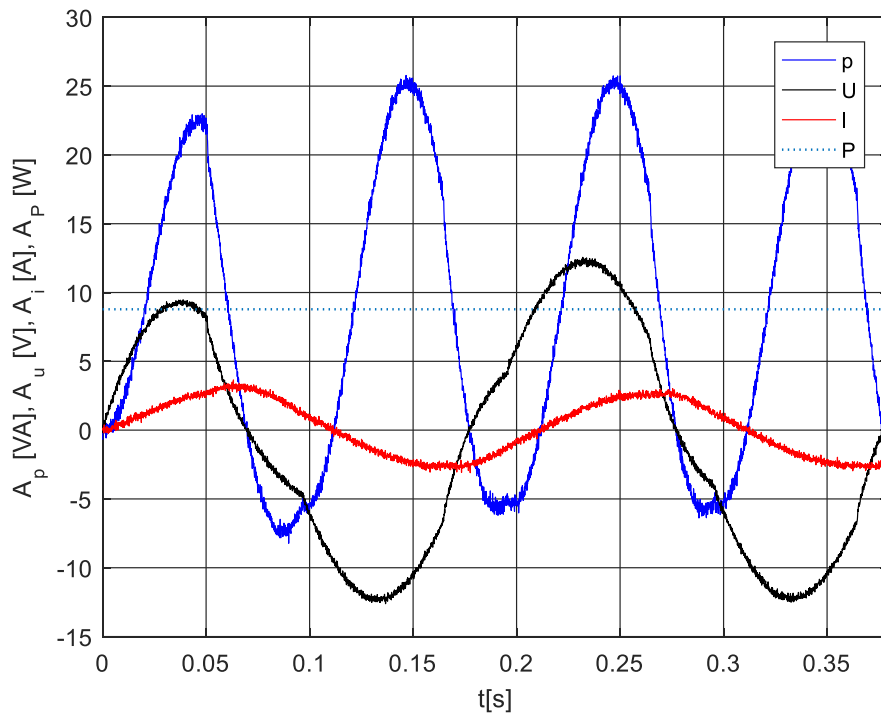
Figure 4: The non-sinusoidal waveforms of voltage, current and powers

1.3 Electric power of currents in three-phase distribution

The highest electric power consumption is happening in a three-phase system. Chapter 1.3 is focused on methods of electric energy consumption, i.e. a three-phase system with balanced and unbalanced load, with sinusoidal and non-sinusoidal currents/voltages.

1.3.1 Electric power of currents in balanced three-phase distribution

Three-phase distribution is performed as four-wired or three-wired distribution. In this case is considered three-phase, four-wired distribution (three wires for phases and one neutral wire), which is described in figure 5 and figure 6.
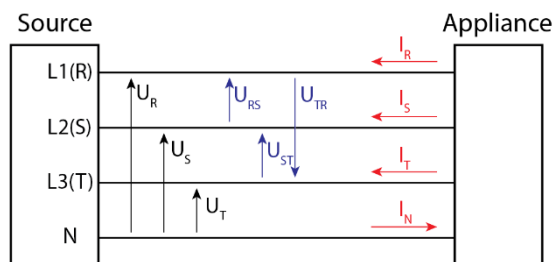
Figure 5: Three-phase distribution with four wires.
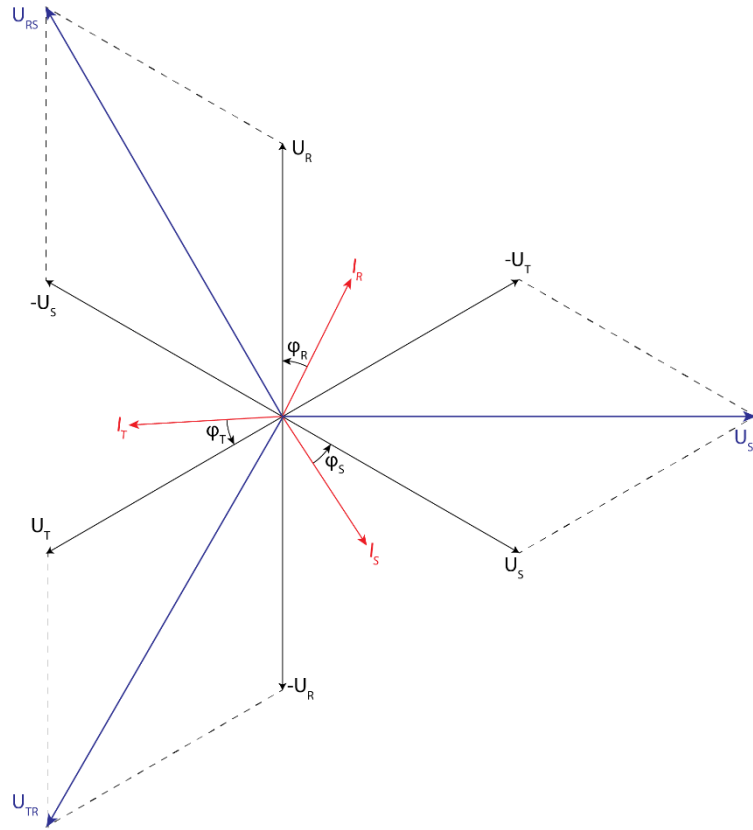
Figure 6: Phase diagram of a balanced system for three-phase distribution with four wires.

From three-phase diagram is obvious, that in four-wired distribution are six different voltages. Three-phase voltages $(\widehat{U}_R, \widehat{U}_S, \widehat{U}_T)$ and three associated voltages $(\widehat{U}_{RS}, \widehat{U}_{ST}, \widehat{U}_{TR})$, where are applied relations:

$$
\begin{aligned}
\widehat{U}_{RS} &= \widehat{U}_R - \widehat{U}_S \\
\widehat{U}_{ST} &= \widehat{U}_S - \widehat{U}_T \\
\widehat{U}_{TR} &= \widehat{U}_T - \widehat{U}_R
\end{aligned}
\tag{11}
$$

These relations are in accordance with second Kirchhoff law. Relations between currents according to first Kirchhoff law looks like:

$$
\hat{I}_R + \hat{I}_S + \hat{I}_T = \hat{I}_N \tag{12}
$$

In the case of three-phase distribution with three wires are different relations, because there is no neutral wire in the distribution. It implies there are only associated voltages $(\widehat{U}_{RS}, \widehat{U}_{ST}, \widehat{U}_{TR})$ and currents, in that case, are in relation:

$$
\hat{I}_R + \hat{I}_S + \hat{I}_T = 0 \tag{13}
$$

In the case of a balanced system are all three phase voltages same values: $\widehat{U}_R = \widehat{U}_S = \widehat{U}_T = \widehat{U}$ which implies that phase of each voltage is shifted by the angle of $\frac{2\pi}{3} => a = \frac{2\pi}{3} = 120°$. This statement is represented by following equations:

$$u_R(t) = \sqrt{2}U_R \sin(\omega t + \alpha)$$
$$u_S(t) = \sqrt{2}U_S \sin(\omega t + \alpha + 2a) \tag{14}$$
$$u_T(t) = \sqrt{2}U_T \sin(\omega t + \alpha + a)$$
$$a + 2a = 2\pi = 0 \tag{15}$$

The phase values of the currents and phase shifts have the same form as voltages

$$\hat{I}_R = \hat{I}_S = \hat{I}_T = \hat{I} \tag{16}$$
$$\varphi_R = \varphi_S = \varphi_T = \varphi \tag{17}$$
$$I_N = 0 \tag{18}$$

The representation of current is represented as the voltage with the same phase shift:

$$i_R(t) = \sqrt{2}I_R \sin(\omega t + \beta)$$
$$i_S(t) = \sqrt{2}I_S \sin(\omega t + \beta + 2a) \tag{19}$$
$$i_T(t) = \sqrt{2}I_T \sin(\omega t + \beta + a)$$

Statements represented by equations (11), (12), (14), (16), (17) are obvious from figure 6, especially is obvious, that values of phase voltages, associated voltages, currents and phase shifts are same. From equation (1) which represents a power of one wave current, we can combine equations for three-phase power.

$$p = u_R(t)i_R(t) + u_S(t)i_S(t) + u_T(t)i_T(t) = p_R + p_S + p_T \tag{20}$$

From equation (20) is calculated active power with using equations (7), (14).

$$P = U_R I_R cos\varphi_R + U_S I_S cos\varphi_S + U_T I_T cos\varphi_T \tag{21}$$
$$U_R I_R + U_S I_S + U_T I_T = A \tag{22}$$
$$P = UI[cos\varphi_R + \cos(\varphi_R + 2a) + \cos(\varphi_R + a)] \tag{23}$$

Reactive power is described by the equation (24):

$$Q = UI[sin\varphi_R + \sin(\varphi_R + 2a) + \sin(\varphi_R + a)] \tag{24}$$
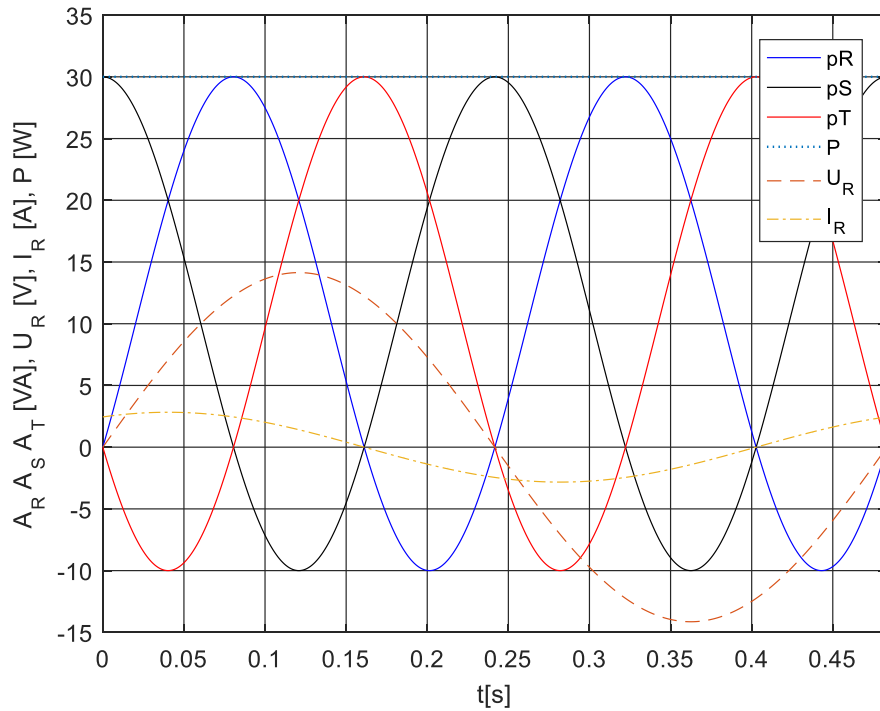
Figure 7: An apparent power of three phases L_R, L_S, L_T and voltage with a current of phase L_R in balanced three-phase distribution.

1.3.2 Electric power of currents in unbalanced three-phase distribution with sinusoidal waveform

In the case of unbalanced three-phase distribution are here considered sinusoidal waves (still linear load). It means that phase shift of each phase has a different value.

$$\varphi_R \neq \varphi_S \neq \varphi_T \neq \varphi \qquad (25)$$

These differences significantly affect the total power distribution, because an active power of each phase can be positive, negative or zero. In this case, currents and voltages of all three phases are same values but generally, in unbalanced distributions, current and voltage of each phase can have a different value, thus:

$$\hat{I}_R \neq \hat{I}_S \neq \hat{I}_T \neq \hat{I}$$
$$\widehat{U}_R \neq \widehat{U}_S \neq \widehat{U}_T \neq \widehat{U} \qquad (26)$$

The power equation for unbalanced distribution is same as for balanced distribution, equations (20), (21). [1]

From figure 8 is obvious, that this phase shift also affects voltage between phases, e.g. $\widehat{U}_{RS} < \widehat{U}_{TR}$. These differences are caused mainly by a different impedance of each phase.
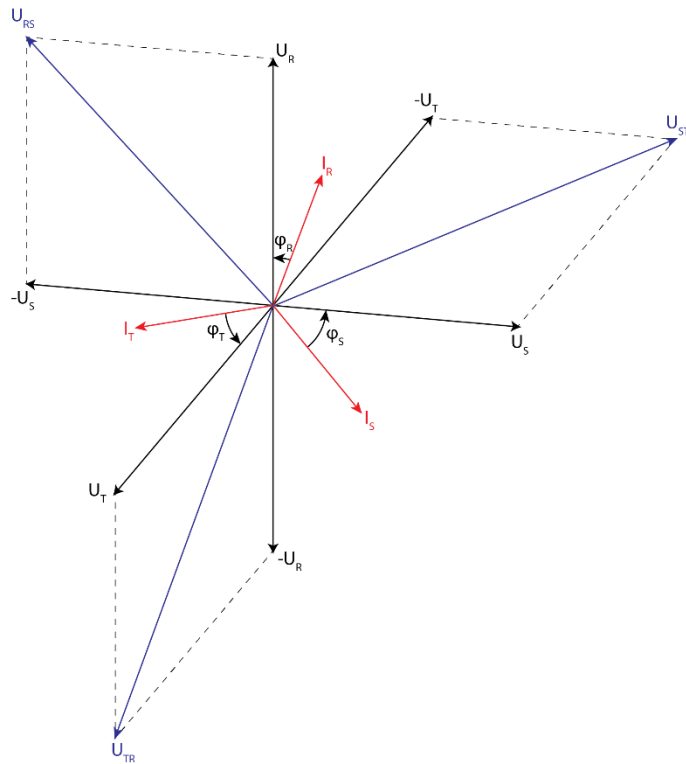
Figure 8: Phase diagram of an unbalanced system with an unbalanced load for three-phase distribution with four wires.

Figure 9: An apparent power of three phases L_R, L_S, L_T and voltage with a current of phase L_R in unbalanced three-phase distribution.

In figure 9 are described apparent power for each phase and sum of active power P. Remember, there are same values of voltage and current for each phase, only difference is in phase shift, due the active power has value: $P = 7.96\,W$ instead of previous 30 W in balanced distribution.

1.3.3 Electric power of currents in unbalanced three-phase distribution with non-sinusoidal waveform

In the past five decades was most common that large electric energy consumption burdens the electric grid by non-sinusoidal currents/voltages and in some cases asymmetrically. These issues are mostly caused by modern technical means of power electronics and different impedance of each phase. In this subchapter will be described electric energy consumption in a deformed three-phase system, i.e. distribution with unbalanced, non-sinusoidal, asymmetrical currents and voltages. This problem can be described same way as in the case of one non-sinusoidal waveform by application of equations (9) and (10).

$$p_{kL}(t_{kL}) = i_{kL}(t_{kL})u_{kL}(t_{kL})\cos\varphi_{kL}(t_{kL}) \tag{27}$$

Index L indicates phase (R, S, T), then the equation for calculating active power is:

$$P = \sum_{L=1}^{3}\left(\frac{1}{n}\sum_{k=0}^{n} i_{kL}u_{kL}\cos\varphi_{kL}\right) \tag{28}$$

This equation can be written as series of equations (numbers of the first sum are changed to the letters because of previous marking):

$$P_R = \frac{1}{n}\sum_{k=0}^{n} i_{kR}u_{kR}\cos\varphi_{kR} = \frac{1}{n}(i_{0R}u_{0R}\cos\varphi_{0R} + \cdots + i_{nR}u_{nR}\cos\varphi_{nR})$$

$$P_S = \frac{1}{n}\sum_{k=0}^{n} i_{kS}u_{kS}\cos\varphi_{kS} = \frac{1}{n}(i_{0S}u_{0S}\cos\varphi_{0S} + \cdots + i_{nS}u_{nS}\cos\varphi_{nS}) \tag{29}$$

$$P_T = \frac{1}{n}\sum_{k=0}^{n} i_{kT}u_{kT}\cos\varphi_{kT} = \frac{1}{n}(i_{0T}u_{0T}\cos\varphi_{0T} + \cdots + i_{nT}u_{nT}\cos\varphi_{nT})$$

Still applies equations (12), (25), (26) which are describing the imbalances in distribution. In three-phase distribution are so-called parasitic non-watt powers (pulsating, hidden, distortion) that accompany the transfer of active power, like reactive power. The main difference is that their mean value is equal to zero, i.e. they are not useful for transfer of energy from the source to an appliance. The presence of these elements increases distribution loss-

es, due to the presence of uncertain current elements. Should be mentioned that this definition is true only in case of undistorted voltage (sinusoidal and without harmonics). Total harmonic distortion (THD) of typical generators is in the distribution on the order of 1-2%, which is slightly larger but it is ignored in common practice. [1]

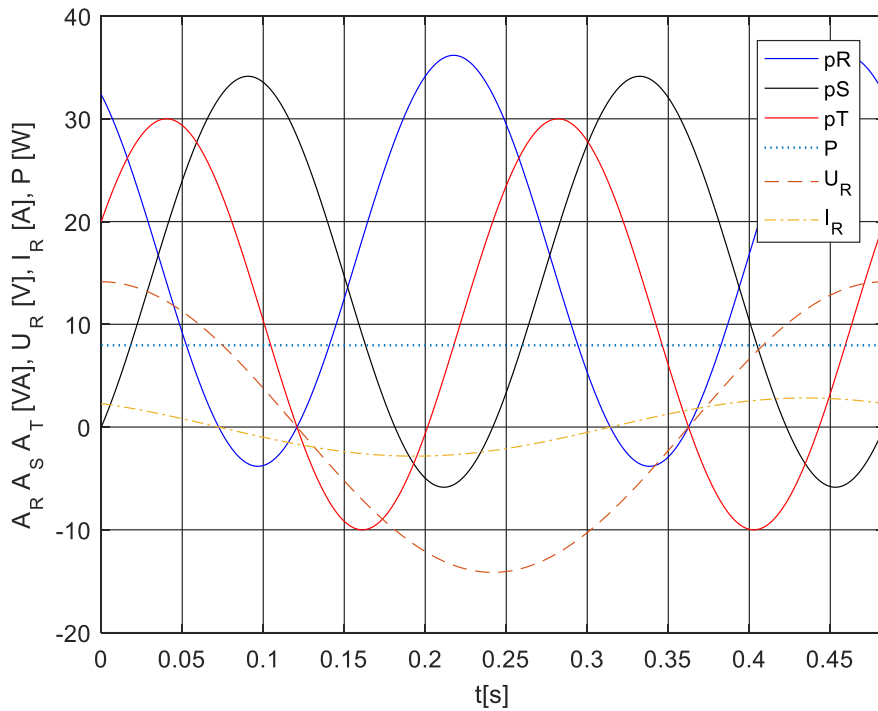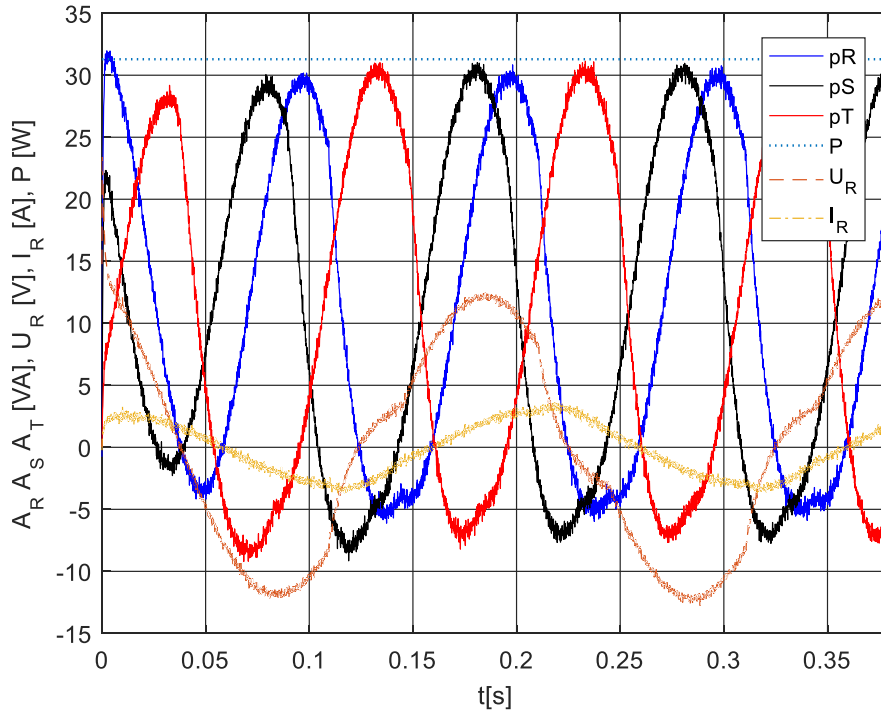Figure 10: An apparent power of three phases L_R, L_S, L_T and voltage with a current of phase L_R in unbalanced three-phase distribution with non-sinusoidal waves.

1.3.4 Often overlooked facts in energy distribution

figure 10 represents three-phase distribution with non-sinusoidal currents and voltages, which is based on equation (28). In truth, waveforms are slightly different due to the different resistance of the wires, which are unknown and in this case were used same values of impedance for each wire. This problem can be described by temperature definition of real active and real apparent power.

$$P_R = \sum_{L=1}^{3} \left(\frac{G}{n} \sum_{k=0}^{n} i_{kL} u_{kL} \cos \varphi_{kL} \right) \tag{30}$$

Coefficient G represents power losses with conductivity from 0 to 1 (parasitic leakage between wires, due resistivity, conductivity and so on). If will be considered real active power due to power losses, then must be changed equation (6) which represents apparent pow-

er. The real value of apparent power (A_{RL}) will include elements such as pulsating, hidden and distortion powers.

$$A_{RL} = \sqrt{P_{RL}^2 + Q_L^2 + P_{PL}^2 + H_L^2 + D_L^2} \tag{31}$$

Where P_P represents pulsating power, H represents hidden power and D represent distortion power. These powers can be described in terms of current and voltage harmonics:

$$\begin{aligned} P_{PL} &= U_{2L}I_{2L} \\ H_L &= U_{3L}I_{3L} \\ D_L &= U_{4L}I_{4L} \end{aligned} \tag{32}$$

Indices 2, 3, 4 indicate the order of harmonics, where first harmonic belongs to active and reactive power (there are a much bigger number of harmonics, which order can theoretically continue to infinity). These parasitic powers can also produce a magnetic field around wires even though the system is purely resistive. Next thing is real power factor which has slightly different value due to distortion power (in compare with the power factor of a balanced system: $cos\varphi = P \cdot A^{-1}$). Then can be written on the basis of the previous statement:

$$\lambda = \frac{P_R}{A_R} = \frac{\sum_{L=1}^{3} \left(\frac{G}{n} \sum_{k=0}^{n} i_{kL} u_{kL} \cos \varphi_{kL} \right)}{\sqrt{P_{RL}^2 + Q_L^2 + P_{PL}^2 + H_L^2 + D_L^2}} \tag{33}$$

Where character: λ represents real power factor of the system which is much more complex and gives more accurate information than $cos\varphi$. This is mentioned from the reason because real power factor assesses more comprehensively the quality of power consumption. [1]

2 TECHNICAL DEVICES FOR ENERGY CONSUMPTION

As was mentioned in chapter 1, electric energy consumption is one of the major problems in world energetics due nonlinearities caused by switching power supplies, frequency converters and so on. All these devices contain rectifier, most usually 6-pulse rectifier, and they draw non-sinusoidal (non-harmonic) current from the electric grid, which leads to the current distortion in the electric grid, power losses, and higher expenses. This deformation effect is called THD – Total Harmonic Distortion which is illustrated in figure 11:
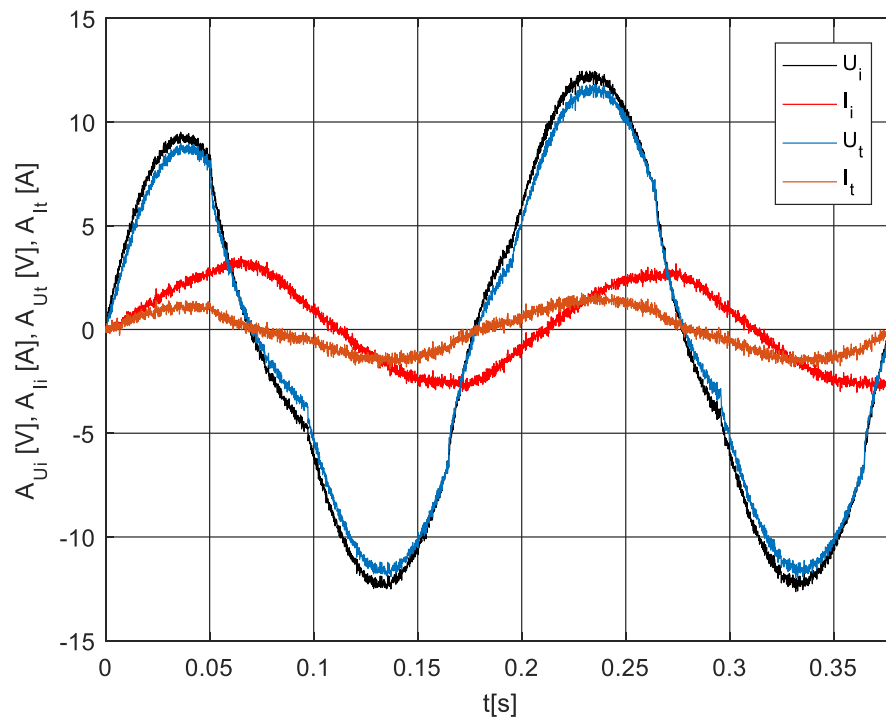
Figure 11: THD of U_i, I_i initial voltage and current to U_t, I_t transformed voltage and current.

For an illustration of THD was used a nonlinear transformer which is causing distortion of voltage and current. Consequently, it is necessary to avoid the THD effect by equipping a system by any harmonic filter with the purpose to mitigate these nonlinearities. [2]

2.1 Harmonic mitigation

There are various harmonic mitigation standards, regulations, and recommendations which sphere of activity depends on geographical areas and industries. Here are commonly encountered standards: IEC61000-3-2 (limits for harmonic current emissions), IEC61000-3-12 (Limits for harmonic currents produced by equipment connected to public low-

voltage systems with input current >16 A and ≤75A), IEC61000-3-4 (Limits, Limitation of emission of harmonic currents in low-voltage power supply systems for equipment with rated current greater than 16A), IEEE519 (IEEE recommended practices and requirements for harmonic control in electrical power systems), G5/4 (Engineering recommendation, planning levels for harmonic voltage distortion and the connection of nonlinear equipment to transmission systems and distribution networks in the UK). Basically, most common way of harmonics mitigation is performed by harmonic filters which are divided into three main categories: passive, active and hybrid. [3]

2.1.1 Passive harmonic filter

Passive harmonic filters consist of capacitors, inductor or a combination of the two in different arrangements. These LC circuits are tuned to each harmonic order to be filtered and are installed in parallel with the non-linear load. This bypass circuit absorbs the harmonics, thus there is avoidance of their flow in the distribution network. Generally, passive filters are tuned close to a harmonic in order to eliminate them (typically 3% to 5% in front of the frequency converter). Several parallel-connected branches of LC elements can lead to a significant reduction of a number of harmonics. [3]
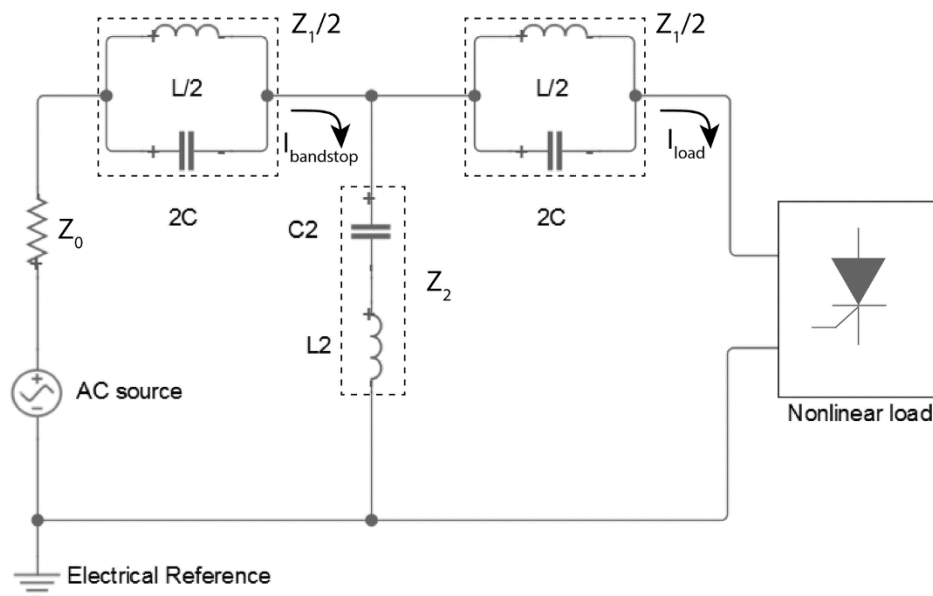
Figure 12: Chebyshev band stop – passive harmonic filter.

figure 12 illustrates passive harmonic filter for one harmonic, also known as Chebyshev band stop filter of sixth order (order of the filter is equal to the sum of reactive components). [4]

2.1.2 Active harmonic filter

Active filters use power electronics switching components to generate currents that mitigate the harmonic currents from a nonlinear load. The active filter investigation in this subchapter is based on a PWM (pulse-width modulation) voltage source inverter that affects the current together with interface filter as is shown in figure 13. In this configuration, the filter is connected in parallel with the nonlinear appliance (thyristor icon). The current from filter effects distorted current from the load and due to it the source current is still sinusoidal. The voltage source inverter used in the active filter is constructed from series and parallels of IGBT (Insulated Gate Bipolar Transistor), DC capacitors as the supply and due to their property to switch at high frequency to generate a signal which will indicate high harmonics. Desired waveform (only voltage) is obtained by accurate controlling of the IGBT switches in the inverter, which is based on the reference between filtered and nonlinear currents. Generated voltage signal from the inverter is received by Interface filter which converts the voltage signal into a current waveform. [5]
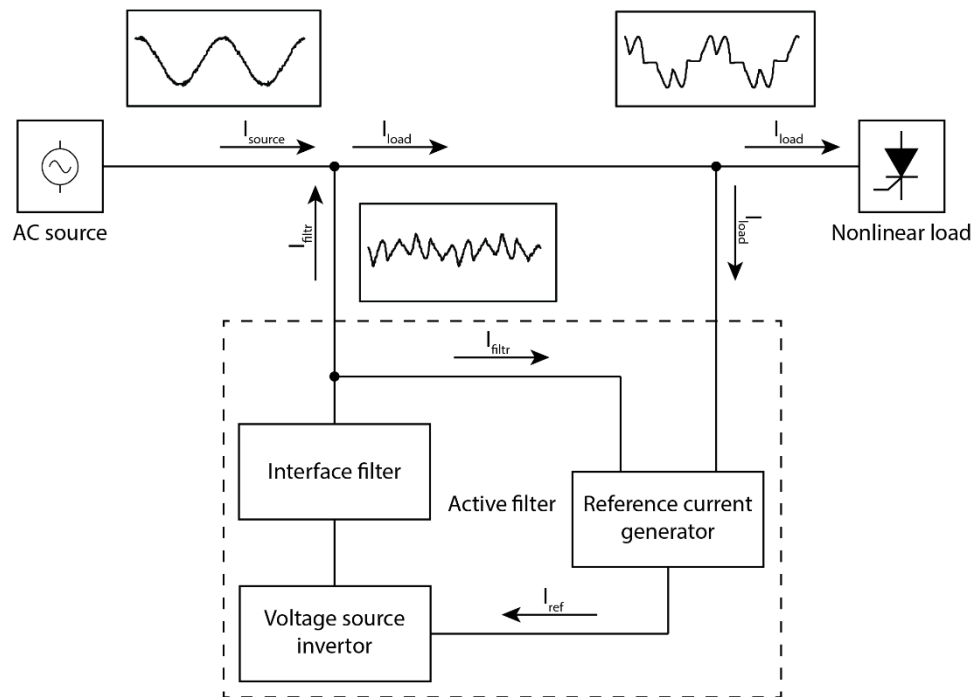
Figure 13: Active harmonic filter with IGBT voltage source inverter. [5]

The simplified model of voltage source inverter is shown in figure 14 (focused on the IGBT connection in H-bridge).
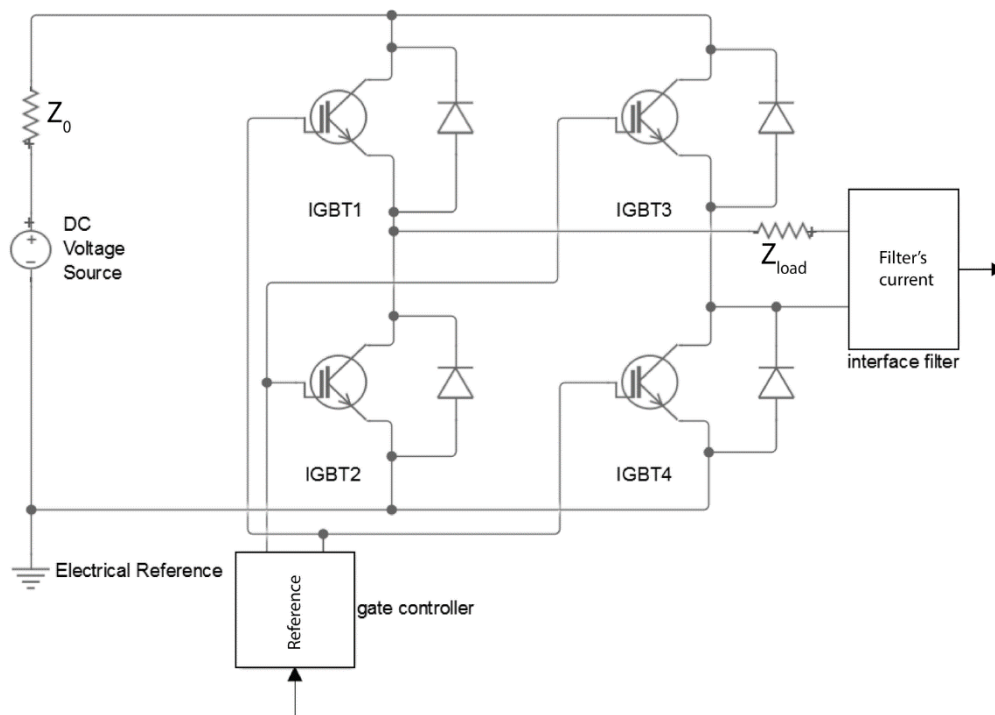
Figure 14: Simplified model of voltage source inverter.

The switches of IGBTs are controlled by gate controller which voltage signals turn on two transistors at ones for possible current flow in the circuit. This IGBTs connection can provide three possible stages of current flow. First is positive square impulse second is the negative and third state is zero. The control signal to gates is basically given by reference signal. This model refers to one phase energy distribution. [8]

2.1.3   Hybrid harmonic filter

Hybrid filters combine the passive and active filter with the purpose to contain the advantages of active, passive filters and lack their disadvantages. They use low-cost high power passive filters to reduce the cost of power converters in active filters. The combination of active and passive filters can vary, thus the power efficiency differs too. In this case, is illustrated Passive shunt active shunt hybrid filter in figure 15. This kind of filter has an active filter in series and a passive filter in shunt. This connection requires slightly bigger power consumption in an active filter, because the passive filter is in parallel. To better performance can be achieved by Passive series, active series combination. Where passive filter is in series and can absorb the maximum of high harmonics. [7]
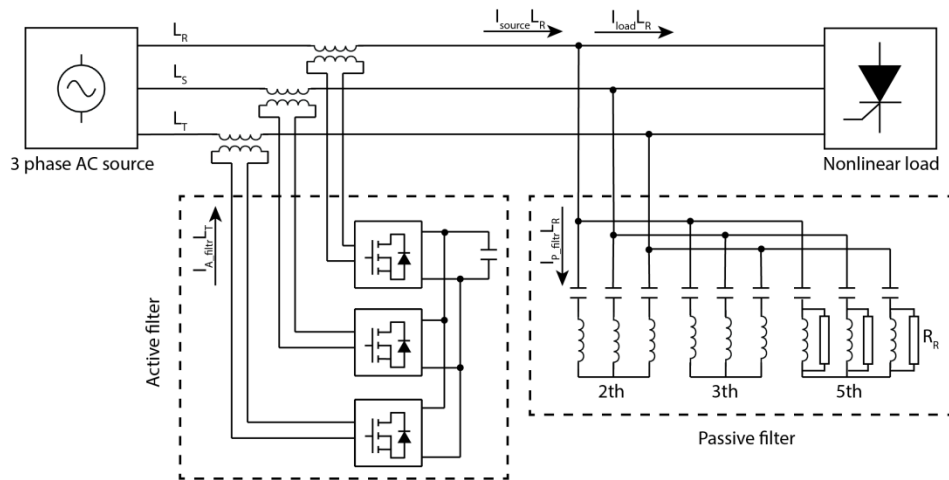
Figure 15: Passive shunt active series hybrid filters. [7]

The passive filter is set to mitigate 2nd, 3rd, and 5th harmonics and thus the energy requirements of the active filter are lower. Figure 15 corresponds to the 3 phase distribution with the wire marks used previously (*R, S, T*).

2.2 Power measuring methods

In this chapter are described basic power measurement methods. These methods can vary in principles which they use (inductance, resistance), usage (AC/DC circuits), connection method (with or without galvanic isolation) and of course in measurement ranges of voltage/current. At last here are mentioned their advantages, disadvantages and simplified mathematical models.

2.2.1 Shunt resistor

It is the simplest and the most accurate method for measurement of current or voltage (depends on the connection). It works on the principle of the different value of voltage/current before the resistor and behind resistor. This principle is described by the equation:

$$U_Z = U - U_m \tag{34}$$

Where known input voltage is U, voltage on the resistor R_n is U_m and voltage behind resistor is U_z. This and more is illustrated in figure 16.
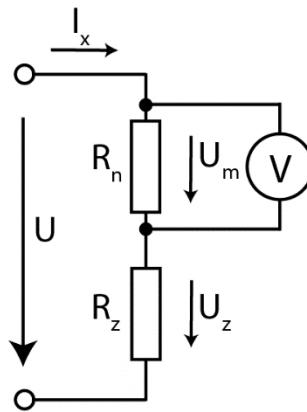
Figure 16: Measuring the current due to the voltage drop. [9]

$$U_m = U \frac{R_n}{R_Z + R_n} = I_x R_n \tag{35}$$

$$I_x = \frac{U_m}{R_n}; \quad i_x(t) = \frac{u_m(t)}{R_n} \tag{36}$$

Resistor R_n is made from wire which resistance is very small and due to it $U_Z \approx U$ (known input voltage). Because of such a small resistance can flow through it a large current (tens of Amperes). The greater resistance R_n causes bigger voltage drop and bigger heat on that resistor which is unwanted. Next advantage of this method is, that can be used for AC or DC circuits. [9]

2.2.2 Measuring transformer

For measurement of alternating current with hundreds of amperes and with high voltage are used current transformers. The main advantage of this method is that the circuit is galvanically isolated from a circuit of high voltage/current and thus the ratio of transferred voltage/current can be scaled. The disadvantages are a bigger size of the device and it cannot be used for DC voltage, due to the transformation which uses electromagnetic induction described by Faraday's law.
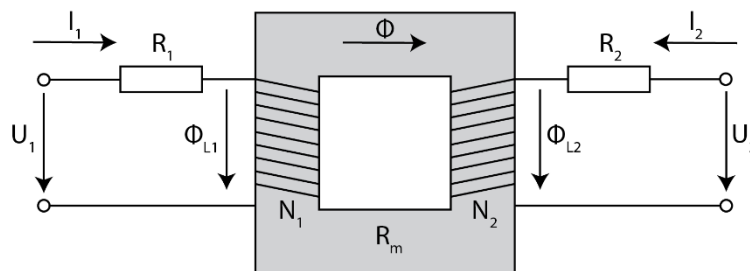
Figure 17: Real transformer. [9]

Here is considered the energy conservation law which can be written as:

$$p_1(t) = p_2(t) + p_a(t)$$
$$u_1(t)R_1i_1(t) = u_2(t)R_2i_2(t) + R_m\phi$$

(37)

Where accumulated power in the core is p_a, the resistance of the transformer core with magnetic flux Φ is R_m. From the Faraday law of induction is known:

$$u_1(t) = N_1\frac{d\phi_{Lr1}}{dt}$$
$$u_2(t) = N_2\frac{d\phi_{Lr2}}{dt}$$

(38)

Where N_1, N_2 are turns ratio of primary and secondary transformer part and Φ_{Lr1}, Φ_{Lr2} are stray magnetic fluxes. Then the voltage part in equation (37) can be substituted by equation (38) and is supposed that both derivation parts are equal.

$$N_1R_1i_1(t) = N_2R_2i_2(t) + R_m\frac{d\phi}{dt}$$

(39)

Then the accumulated voltage in the core can be calculated:

$$u_m(t) = \frac{d\phi}{dt} = \frac{1}{R_m}(N_1R_1i_1(t) - N_2R_2i_2(t))$$

(40)

And current on the secondary site:

$$i_2(t) = \frac{1}{N_2R_2}\left(N_1R_1i_1(t) - R_m\frac{d\phi}{dt}\right)$$

(41)

2.2.3 Hall sensor

This method uses magnetic sensors/hall sensors, located in air gaps of a magnetic circuit and with an amplifier as feedback. The measurement principle is based on Biot-Savart's law which is describing magnetic field around the wire due to the current flow in a certain distance. This principle can be described by the equation:

$$AC: \quad \phi(t) = \frac{\mu_0 r^2}{2(l^2 + r^2)^{\frac{3}{2}}}i_x(t)$$
$$DC: \quad \phi = \frac{\mu_0 r^2 I_x}{2(l^2 + r^2)^{3/2}}$$

(42)

Where l is certain, measured distance, r is a radius of the wire, $i_x(t)$ is the actual value of flowing current in that certain distance and $\mu_0 = 4\pi \cdot 10^{-7}\ NA^{-2}$ is magnetic constant. From equation (38) is known that:

$$u(t) = \frac{d\phi}{dt} \quad or \quad i_x(t) = \frac{2(l^2 + r^2)^{3/2}}{\mu_0 r^2}\phi(t) \tag{43}$$

Hall sensor using this principle is illustrated in the following figure. [10]
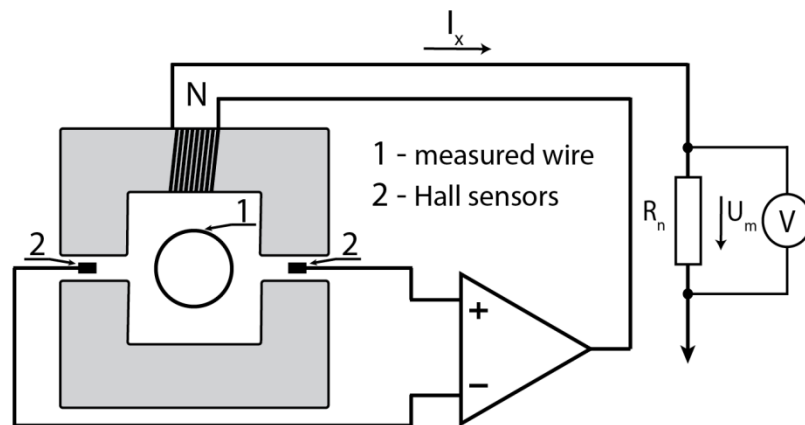
Figure 18: Hall sensor with a converter for current measurement. [9]

In addition, in this circuit is compensation coil (*N*), which by own polarity mitigates magnetic flux of primary wire. The current flows through shunt resistor which is in combination with hall sensor. As should be seen on the previous page, this method can be used for DC and AC power measurement which is one of many advantages. Next advantages are that this method can be used in frequency specter till tens of *kHz*, has a low heat drift, good linearity, and excellent accuracy. [9]

3 MEASURING DEVICES OF ENERGY CONSUMPTION

On the market is a plethora of measuring devices for energy consumption that is not possible to describe them all. This chapter is focused on those devices which are most known and most used in practice in past years. Generally measuring devices can be divided on the basis of their physical principle (inductance, resistance …), the form of current (AC/DC), analog/digital evaluation and since new millennium of their part composition (static/dynamic – uses movable parts).

3.1 Watt and energy meters

Simply said, power meter measures the rate at which work is performed or energy is transmitted in a certain moment which explains physical unit Watt [W] where is known $1W = 1J \cdot s^{-1}$. Against it, energy meter measures consumed power over a time interval thus it is expressed in terms of Watt-second [Ws], Watt-hour [Wh] or kiloWatt-hour [kWh] for convenience. This statement can be presented by equation (44) for analog energy meters and in a case of digital energy meters, must be used sampled time (T) and integral is then replaced by the sum, equation (45). [11]

$$E = \int_0^t p \, dt = \int_0^t u \cdot i \, dt \tag{44}$$

$$E = \sum_{k=0}^N p_k = \sum_{k=0}^N u_k \cdot i_k \tag{45}$$

The main difference between Watt meters and energy meters is that energy meters should sum and store the measured values. Against it, Watt meters are only showing the actual value of electric power, but essentially the measuring principle of energy or power is for both physical quantities similar. [11]

3.2 Analog and digital energy meters

3.2.1 Analog energy meters

Analog meters do not use exact power/energy measuring methods mentioned in chapter 2.2 but are still based on the same physical principles. Most of an analog energy meters are inductive, it means that measurement is evaluated on the basis how much current/voltage is inducted in measuring coils and then this current/voltage is displayed by certain way. The principle of analog measuring is simply described in figure 19.
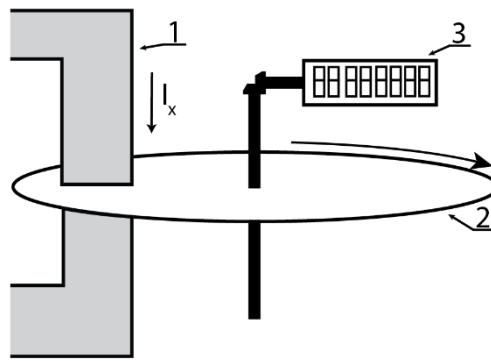
Figure 19: Principle of analog induction energy meter.

Through coil core (1) the induced current (I_X) flows which affect the disc (2) and make it rotate. Each rotation period is transferred through gears to a counter (3). For example, an analog meter can be almost same as one, which is described in figure 21 (chapter 3.3), but without the rotation sensor, which is used for further digitalization. Analog energy meters are still widely used but in future should be completely replaced by digital (solid-state) energy meters because of the trend of automatization and their better properties.

3.2.2 Digital energy meters

The main difference against analog energy meters is that digital meters need AD converter and microcontroller for further computing operations. AD converter samples the analog, continuous signal to samples which are further processed by a microcontroller. In this case, IN1 and IN2 can represent measured values of voltage and current which are amplified by PGA, processed by microcontroller and transferred to out as a signal.
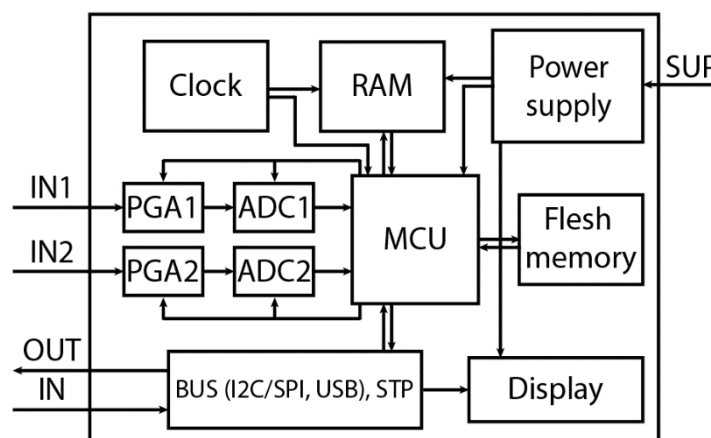
Figure 20: Principle of digital energy meter.

Although due the sampling is lost a part of the analog information, there are still various advantages of digital energy meters against analog. The main advantage is probably that

digital energy meters can detect distortion of the measured current and voltage and thus the microcontroller can calculate real power factor, a percentage of current/voltage distortion, real apparent power, they have higher accuracy and so on. Most today used digital energy meters are based on physical principles mentioned in chapter 2.2.

3.3 Dynamic and static energy meters

3.3.1 Dynamic energy meters

These dynamic electrometers are also cold electromechanical meters (consists of moving parts like switches, relay, rotor …). What is more important, they have almost no usage in automatization, because of their properties (bigger size, slow sampling because of the moving rotor, low reliability, cannot register distortion …).

For clarity is here described galvanically isolated electromechanical induction meter for one phase:
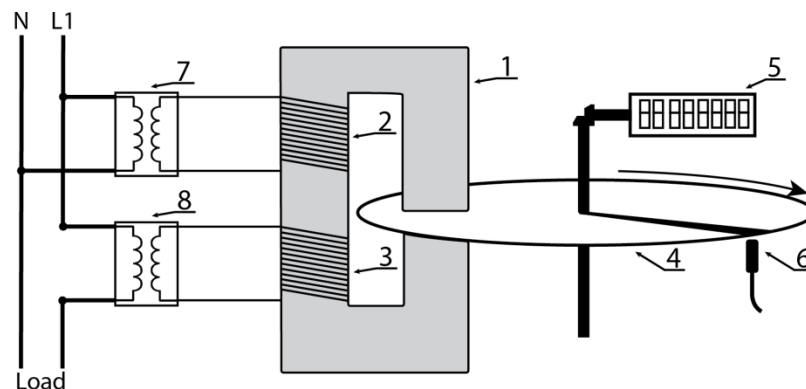
Figure 21: One-phase electromechanical induction energy meter. [12]

Important to note, this energy meter is only for measuring AC power/energy as was previously written about induction meters. The principle is following. Through inductive system with a gradual magnetic field (1) is flowing current created by current coil (3) and voltage coil (2) which create an electromagnetic field. Both of these coils are separated from the phase by transformers (7), (8), which reduce/increases the incoming voltage/current. Created magnetic circuit is connected through aluminum disc (4), where is induced eddy current which is causing torque of the disc. This torque is linear to the immediate power represented by modified equation (7) into equation (46).

$$m(t) = \frac{k}{T} \int_0^T u(t)i(t) \; dT \tag{46}$$

Where a constant of energy meter is k. Then the torque for active power is given by equation (47) for ideal waveform (balanced load, sinusoidal AC voltage, and current).

$$M = k \cdot UIcos\varphi \tag{47}$$

The rotation of the disc is converted to the counter (5) (which displays the total consumed energy) or to impulses by the rotation sensor (6). The value of power is then given by frequency of disc rotation and consumed energy is calculated based on speed of rotation. Impulses from the sensor can be processed by microcontroller and stored in memory. [12]

3.3.2 Static energy meters

Static energy meters are on the market past 10-20 years and they are purely digital, without moving parts like rotor, relays, switches and so on. The measured current and voltage are computed by microcontroller and the following sum and other parameters are displayed on LCD or LED display or can be sent through analog I/O to another device (PLC, IPC …) as current/voltage signal of certain range $(e.g. \, 0 - 10V, 4 - 20mA)$. Figure 22 represents basic power evaluation in digital energy meter (using transformers).
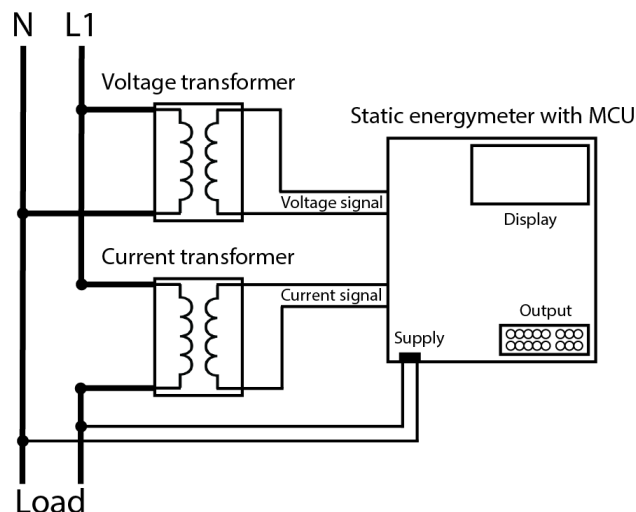
Figure 22: Basic diagram of power evaluation by microcontroller in static energy meter for one phase. [13]

Measured voltage and current are processed through ADC by MCU. Measured signals can be displayed or can be read through BUS, GSM and so on (depends on the architecture).

4   VOLUMETRIC/MASS FLOW RATE

Generally, there are two types of flow rate, volumetric and mass flow rate. The difference is just in physical principle which will be described in following chapters. Basically, flow rate in physics, fluid dynamics and hygrometry is synonymous for electric current in electronics, electro-technics and so on (generally: flow of particles in time). Mass/volume flow rate must be caused by something like as voltage cause flow of electric current. This something is pressure (force acting on the mass/volume).

4.1   Ability to flow

Ability to flow has just some substances, generally known as liquids and gasses. This must be distinguished for measuring because certain types of measuring devices can be inappropriate for measuring of gasses, but appropriate for liquids. [15]

4.1.1   Liquids

Liquids are substances without specific shape in liquid state, in this form the particles are relatively close to each other (form drops), but they are not rigidly bound by force and due to it they can move in their whole volume. The important phenomenon is that liquids cannot hold a shape without a vessel. Other phenomena are: they are practically incompressible, retain the same volume, maintain the water-level, differs in viscosity and they conduct an electric current. [15]

4.1.2   Gasses

As liquids, gasses are also substances without specific shape with difference in state of aggregation. Substances in gas state contain particles, which are relatively far from each other and they are not rigidly bound by force. Same as liquids, gasses cannot hold a shape without a vessel. The main differences against liquids are: Gasses are compressible, they do not retain in the same volume (always fill a whole vessel). They conduct an electric current only in certain condition (must consist of free particles with electric charge). Since 19th century the gasses are divided into two groups: ideal and real gas models. [15]

Ideal/perfect gas

Can be described as substance which contains numerous, small particles, which are in constant motion, but still, they do not force on each other. This ideal/perfect gas can be described by ideal gas formula (very simplified):

$$P \cdot V = n \cdot R \cdot T \tag{48}$$

Where P is the pressure, V is the volume, n is amount of gas (in molar units), $R = 8.3144 \, J \cdot K^{-1}$ is the universal gas constant and T is the temperature in Kelvins. [15]

Real gas

Properties of these gasses are different from ideal gasses. Between the particles of these gasses are different forces, which are causing liquefaction. For real gas is necessary to take into an account its molar weight and molar volume (one mole of a substance at a given temperature and pressure). Then the equation for pressure looks like:

$$P = \frac{RT}{V_m - b} - \frac{a}{V_m^2}$$

$$V_m = \frac{RT}{P}; a = \frac{27R^2 T_c^2}{64P_c}; b = \frac{RT_c}{8P_c} \tag{49}$$

Where b and a are specific parameters for each gas, T_c is critical temperature, P_c is critical pressure. T_c and P_c together define a critical point at which the gas liquefies. [14]

4.2 Volumetric flow rate

The volumetric flow rate is given by the volume of fluid V through a surface per unit time t. It can be written as:

$$\dot{V} = \frac{dV}{dt} \tag{50}$$

This volumetric flow rate obviously depends on velocity v of the flowing particles through certain area S, then the equation (50) can be rewritten as:

$$\dot{V} = v \cdot S = S\frac{dl}{dt} \tag{51}$$

Where the length is l, the certain area is S through the particles flow. For gasses are applied equations (48) and (49). [15]

4.3 Mass flow rate

The mass flow rate is given by the mass m of a substance which passes per unit of time t, which can be represented by the following equation:

$$\dot{m} = \frac{dm}{dt} \tag{52}$$

Mass flow can be also calculated from volumetric flow rate, based on the following equation:

$$\dot{m} = \dot{V} \cdot \rho = v \cdot S \cdot \rho \tag{53}$$

For gasses, the mass flow is given by conversion of volumetric flow rate, based on density of certain gas. This conversion is more problematic due to the temperature and pressure changes. It is necessary to continuously measure these values and in some cases measure substance composition of the gas. Usually, are used nominal flow rate (absolute pressure 101.325 kPa and temperature $0°C$). The calculation of ideal/perfect gas mass flow rate is based on density (very simplified):

$$\rho = \frac{MP}{RT} \tag{54}$$

$$\dot{m} = \dot{V} \frac{MP}{RT} = v \cdot S \frac{MP}{RT} \tag{55}$$

The equation (54) is describing the mass flow rate of the flowing particles in the system which are dependent on molar mass $M \ [kg \cdot mol^{-1}]$, pressure, temperature, their velocity and surface of the vessel. [15]

5 FLOW SENSORS AND FLOW METERS

In this chapter is described difference between flow sensors and flow meters, basic distribution of them, because there are so many aspects which can affect the measurement. Another fact is that this topic is extensive and goes beyond cope of this master thesis. For that reason will be listed only those basic and mostly used flow sensors and flow meters.

5.1 Flow sensors

Flow sensors transform measured values of flow rate to another physical quantity, which is related to velocity of the substance or with its kinetic energy. Flow sensors can be divided into groups based on:

Measured physical quantities:

1) Mass flow
2) Volumetric flow

Type of flow:

1) Laminar flow – predominates effect of friction forces between mutually non-mixed layers of the flowing fluid
2) Turbulent flow – The particles cross runways of each other which generate vortices and chaotic move of fluid (does not contribute to their flow).

The method of measurement:

1) Direct – dosing sensors, pumps (divides the fluid into strictly-defined portions and transport them in direction of flow). The principle is based on volumetric flasks, which are periodically filled and emptied by flowing fluid with contribution of kinetic energy.
2) Indirect – most of the measurements are based on difference of output measured value and input measured value (kinetic energy or velocity). [15]

5.2 Parameters of flow sensors/flow meters and their correct selection

For both: flow sensors and flow meters are important their parameters because there is no universal flow sensor/meter for sensing/measuring both: liquids and gasses in every environment. Due this is necessary to distinguish and respect all influences which can cause inaccurate sensing/measurement. Basically, should be distinguished:

1) Process – continuous/discrete, linear/nonlinear, one-time/permanent/repeated, industrial/laboratory/hobby, …

2) Kind, properties and volume/mass of measured medium – liquid/gas, their viscosity, temperature, aggressiveness, pressure, …

3) Kind and properties of measured place – conduit/open canal, their shape, size, …

4) Parasitic influences – pressure loss, vibration, temperature change, …

5) Accuracy (uncertainty of measurement) – for flow meters with/without correction.

6) Material wear – moving/static parts.

7) Dynamic properties – time constant, time delay.

Particularly high demands are placed on uncertainty of measurement of measured medium/fluid. Another demand depends on the environment where the flow sensor/meter is used. In industrial environment are required high demands on reliability and resistance against parasitic influences (vibration, dust resistance). [15]

5.3 Flow meters

The principle of flow meters is conversion of measured physical quantity to analog or binary data. In most cases are measured volumetric and mass flow rate, which are based on fluid flow. Highly discussed topic around flow meters is accuracy and usage which depends on used sensor and its properties (chapter 5.2). These parameters will be described for each type of flow meter.

5.3.1 Venturi tube

Venturi tube uses simple principle based on pressure difference based on Bernoulli differential equation (The principle of maintaining energy in the flowing fluid). This statement can be represented as:

$$p_1 + \frac{1}{2}\rho V v_1^2 = p_2 + \frac{1}{2}\rho V v_2^2$$
$$p_1 - p_2 = \frac{\rho V}{2}(v_1^2 - v_2^2)$$
(56)

Then in the equation (56) can be velocity $v_{1,2}$ substituted if is applied equation:

$$\dot{V} = S_1 \cdot v_1 = S_2 \cdot v_2$$
$$v_2 = \frac{v_1 S_1}{S_2}$$
(57)

The result of the previous statement is:

$$\Delta p = \frac{\rho V}{2}\left[v_1^2 - \left(\frac{v_1 S_1}{S_2}\right)^2 \right]$$

$$\frac{2\Delta p}{\rho V} = v_1^2 \left[1 - \left(\frac{S_1}{S_2}\right)^2 \right]$$

$$v_1 = \sqrt{\frac{2\Delta p}{\rho V} \cdot \frac{1}{\left[1 - \left(\frac{S_1}{S_2}\right)^2 \right]}} \tag{58}$$

$$\dot{V} = S_1 \sqrt{\frac{2(p_1 - p_2)}{\rho V} \cdot \frac{1}{\left[1 - \left(\frac{S_1}{S_2}\right)^2 \right]}}$$

Where cross section and pressure in conduit are S_1, p_1, cross section and pressure in narrowed part of Venturi tube, density and volume of the fluid in the conduit/Venturi tube are $S_2, p_2. \rho, V$. [16]
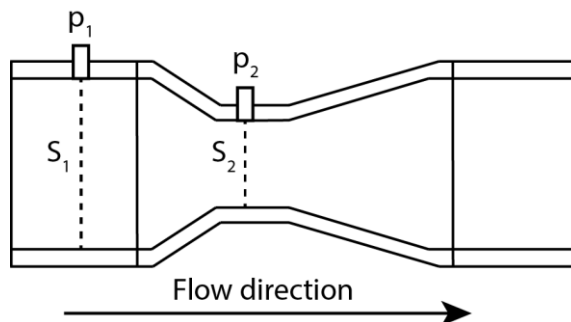
Figure 23: Venturi tube.

The main disadvantage of the Venturi tube is pressure loss due the narrowing. If the Venturi tube is used for measuring of large flow of high viscosity liquid, then is usual large wear of its material. On the other hand, Venturi tube has good accuracy (1-2% uncertainty of measurement) and can be used for various liquids and gasses with pressure up to $41 MPa$. [15]

5.3.2 Hot-wire

Hot-wire is one of many flow sensors based on the thermal principle which is most common method used to measure instantaneous fluid velocity. The technique depends on the convective heat loss to the surrounding fluid from an electrically heated sensing ele-

ment or probe (usually wire). The heat loss changes with changing velocity of the fluid and the principle is suitable for both: turbulent or laminar flow.

Figure 24: Hot-wire.

Between two probes (2) located usually in ceramic isolation (3) is stretched resistive wire (1) of small diameter which is heated by electric current above temperature of surroundings (usually $5\mu m$ Pt, Pt-Ir wire). This thermal process can be described by the following equation:

$$I^2 R = K\lambda Pr^k Re^n S\Delta T \tag{59}$$

Where flowing current in the wire is I, heated resistance wire is R, proportionality constant is K, thermal conductivity of the fluid is λ, Prandtl's dimensionless number is Pr, Reynold's dimensionless number s Re , k and n are experi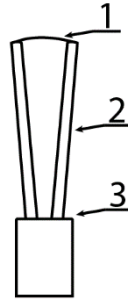ment constants, S is outer surface of the heated resistive wire and ΔT is temperature difference between heated resistive wire and a flowing fluid. Reynold's dimensionless number is described as:

$$Re = \frac{vl\rho}{\eta} \tag{60}$$

Where v is velocity of flowing fluid, l is characteristic dimension of the wire along the fluid flow (usually length of the wire), ρ is density of the fluid and η is dynamic viscosity. Then the equation (60) can be applied to equation (59) with result in equation (61) known as King's equation. The latest step is to express velocity v of the flow through the surface.

$$\dot{V} = S \cdot v = \frac{\eta}{l\rho} \cdot \sqrt[n]{\frac{I^2 R}{K\lambda Pr^k \Delta T}} \tag{61}$$

Should not be forgotten, this kind of flow meter must be calibrated first because of the initial flow state. Usually, is used for this purpose another flowmeter. If hot-wire flow meter is correctly calibrated then can be achieved really good accuracy (uncertainty of measurement since 0.1% till 0.5%). Additionally, they dispose of high sensitivity, low-pressure

loss, and low time delay. They can be used in pressure conditions up to 100 MPa with temperature range since -200 °C till 400 °C. [15]

5.3.3 Ultrasonic flow meter

On the market are several types of ultrasonic flow meters which are working on different principles (source-reflector, source-emitter and so on). Here will be described the source-emitter version which is based on time difference between generated and received ultrasound signal. The time difference is affected by flow of the fluid. If the signal is generated against the fluid flow the time difference is higher than in case of the generated signal on the direction of fluid flow.
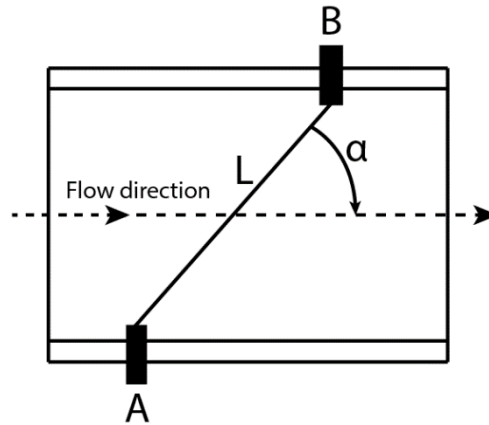
Figure 25: Ultrasonic flow meter.

Where A and B are ultrasonic transducers, L is vector length of the ultrasonic signal between transducers and α is the angle between vector of ultrasonic signal L and vector of flowing fluid direction. From the figure 25 is obvious that velocity of ultrasonic waves, in direction from transducer A to transducer B, with velocity of electromagnetic waves c_0 can be described as $c_0 + v \cdot cos\alpha$. In opposite direction the velocity will be $c_0 - v \cdot cos\alpha$, then the time differences can be estimated as:

$$t_1 = \frac{L}{c_0 + v \cdot cos\alpha}$$

$$t_2 = \frac{L}{c_0 - v \cdot cos\alpha}$$

(62)

$$\Delta t = t_2 - t_1 = 2L \frac{v \cdot cos\alpha}{c_0^2}$$

$$v = \frac{\Delta t c_0^2}{2L \cdot cos\alpha}$$

(63)

This kind of measurement is affected by viscosity and density of the fluid which is dependent on Reynold's number (may differ for laminar or turbulent flow) and so affects the form of equation (51):

$$\dot{V} = S \cdot \frac{v}{k} \tag{64}$$

$$k = 1 + \frac{0.295}{1.2 \cdot \ln(Re) - 1} \tag{65}$$

Where the constant dependent on Reynolds dimensionless number is k. At the end, equation (63) can be applied to equation (64).

$$\dot{V} = S \cdot \frac{c_0^2 k \Delta t}{2Lcos\alpha} \tag{66}$$

Between the main advantages belongs its universal use (usable for liquids and gasses including water vapor). It can works in any position with different diameters of conduit (range from 12 mm to 6 m). There is almost no pressure loss and the measurement is not affected by fluid content (bubbles, or solid elements). The volumetric flow rate range is from 2 to 400 000 m^3h^{-1} up to pressure of 100 kPa with temperature range from -300 °C to 600 °C. Uncertainty of measurement can differ due to the diameter of conduit. For correct measurement with uncertainty of measurement 2% is necessary to use calming conduit (*15D* before device and *5D* behind the device, where *D* is diameter of the conduit). [15]

II. ANALYSIS

6   MEASURING DEVICES OVERVIEW

In this chapter are described industrial energy meters and flow meters which can be applied for given purpose. In every welding cell is PLC for automatization tasks and the goal is to use it for collecting of measured data and following operations. It means that reviewed measuring devices have to be digital and in the best case with digital and analog outputs or BUS communication. At last measuring devices should dispose of satisfying accuracy and good reliability.

6.1   Overview of selected energy meters

6.1.1   Energy meter ABB A43 212-100

Key applications:

- Applications in industry,
- Applications in commercial buildings,
- Object metering,
- Billing applications.

Meter performance:

- Three phase and single phase measurement,
- Mounting system: DIN, Protection class: IP 20,
- Direct connected up to 80 A and transformer connected: 1, 2 or 5A,
- Voltage range (100 - 500V),
- Recording of active or active and reactive energy,
- Accuracy class: CI.1, Class B - (1% - 2%),
- Communication via RS-485 with pulse output. [17]

Figure 26: Energy meter ABB A43 212-100. [17]

6.1.2 ET 200SP AI Energy Meter 400VAC ST

Key applications:

- Application in industry (suited for production machines).

Meter performance:

- Three phase and single phase measurement, Protection class: IP20,
- Maximum permissible AC current: 5 A, transformer connected: 1 or 5A,
- RMS voltage range: 100 - 400V,
- Accuracy of $\pm0.5\%$ with balanced load,
- Recording of voltages, currents, phase angles, powers (active, reactive and apparent), energy values, frequencies,
- Supports firmware updates and reconfiguration in RUN through STEP7 or TIA portal V13,
- Communication through PROFINET and PROFIBUS. [18]

Figure 27: AI Energy Meter 400VAC ST with AI module. [18]

6.1.3 Schneider Electric PM3250 Power Meter

Key applications:

- Buildings,
- Industry,
- Data centers and networks,
- Infrastructure (airports, road tunnels, telecom).

Meter performance:

- Three phase and single phase measurement,
- Mounting system: DIN, Protection class: IP20,

- Maximum permissible AC current: 5 A, transformer connected: 1 or 5A,

- RMS voltage range: 80 - 570V,

- Accuracy of $\pm 0.5\%$ with balanced load,

- Recording of voltages, currents, phase angles, powers (active, reactive and apparent), energy values, frequencies, THD,

- Records Min/Max of the instantaneous values

- Communication through RS-485 port for Modbus communication. [19]

Figure 28: Schneider Electric PM3250 Power Meter. [19]

6.1.4 Evaluation of reviewed energy meters

Based on introduced energy meters in previous subchapters was chosen for further use AI Energy Meter 400VAC ST. The main reasons are:

- In welding cells is used PLC Simatic S7-1500 from Siemens including all other components and software like ET200SP I/O station, power source and other peripherals.

- Better price for AWL-Techniek (comparing with other two reviewed energy meters).

6.2 Overview of selected flow meters

6.2.1 Testo 6443

- Industry application,

- Process pressure up to 16 Bars and humidity up to 90%,

- Protection class: IP64, for pipes of DN40,

- Analog output: current with range 4-20 mA,

- Accuracy of 3%,

- Minimum flow: 22 l/min, maximum flow: 6667 l/min. [20]

Figure 29: Flow meter Testo 6443. [20]

6.2.2 Aventics AF1 series

- Industry application,

- Process pressure up to 16 Bars and humidity up to 90%,

- Protection class: IP65,

- Analog output: current with range 4-20 mA or voltage with range 0-10V DC,

- Accuracy of 3%,

- Product codes: R412010638 (voltage output) or R412010673 (current output),

- Minimum flow: 150 l/min, maximum flow: 2000 l/min. [21]

Figure 30: Flow meter Aventics. [21]

6.2.3 Festo SFAM 62 flow sensor

- Industry application,

- Process pressure up to 16 Bars and humidity up to 90%,

- Protection class: IP65,

- Analog output: current with range 4-20 mA or voltage with range 0-10V DC,

- Accuracy of 3%,

- Product code: 564940, SFAM-62-5000L-M-2SV-M12 (voltage output),

- Minimum flow: 50 l/min, maximum flow: 5000 l/min. [22]

Figure 31: Festo SFAM flow sensor. [23]

6.2.4 Evaluation of reviewed flow meters

In this case was chosen for further use Festo SFAM flow sensor from sensors which are introduced in previous subchapters. The decision is based on several reasons. Main of them is that the welding cells are using all pneumatic devices from Festo Company and this flow meter/sensor should be easily implemented between them and it costs half of the money (for AWL-Techniek) in compare with the other mentioned flowmeters. The second reason is that mounting of flow meter/sensor is made for hose pipes of DN11 and pressure of 6 bars (there is not necessary the hose pipe resizing).

7 INTEGRATION OF MEASURING DEVICES INTO THE WELDING CELL

This chapter is focused on implementation of measuring devices into the welding cell. As first will be described basic idea how the measurement system will be set up, what devices are necessarily required for it and possible extension in the future. In the second part will be shown a picture of welding cell where will be highlighted positions of devices required for energy measurement system.

7.1 Required devices for energy measurement system and their connections

Based on the chosen measuring devices and their properties are necessary to include additional devices (current transformer, AI module for Festo flow sensor) to the measuring system design. A simple diagram of the measuring system with visualization is described in the following figure.

Figure 32: Simple diagram for energy consumption measurement and visualization.

The current transformer (4) is connected to the main power lines at the input of the welding cell in the main switchboard. A current transformer is necessary because energy meter can work with the maximum current of 5 amperes and through the main power lines can flow up to 60 amperes. On the other hand, there is no need of voltage transformer because the welding cell is connected to the power source (1) of 400 VAC to which the energy meter can be connected directly. Measured data of voltage, current, and flow are dis-

tributed as analog output from measuring devices to the ET I/O station and PLC (2) which performs all mathematical and logical operations. The communication of PLC with HMI (6) panel of the cell (for visualization) is performed through Profinet. Communication for PLC with programming PC (5) is same (through Profinet).

In additional, the project is prepared for possible extension in the future because for a customer is more comfortable to start any web browser and check the energy consumption from home, office, bus stop or from somewhere else. It could be done by connecting the PLC with router (7) which can communicate through internet/WAN (10) with web server (9).

Table 1: Additional devices for energy measurement overview.

Device	Manufacturer	Type	Code
Flow meter	Festo	SFAM-62-M	SFAM-62-5000L-M-2SV-M12
Base unit for Energy meter	Siemens	400V AC	6ES7193-6BP00-0BD0
Energy meter	Siemens	AI Energy Meter ST	6ES7134-6PA01-0BD0
Base unit for ET AI module	Siemens	24V DC/10 A	6ES7193-6BP00-0DA0
ET AI module	Siemens	AI 4xU/I 2-wire ST	6ES7134-6HD00-0BA1
Current transformer	Siemens	AC 3x100/5 A	7KT1201

Important to note, that table 1 does not include existing devices which are already used for other purposes in the welding cell. Block diagram of the AI energy meter ST and Flow meter can be found in appendix 1 and connection of the flowmeter in appendix 2.

7.2 Placement of energy measurement system components in the welding cell

Placement of energy measurement system components was tested on one specific cell for Johnson Controls. In any case, AWL Techniek is constructing many variants of welding cells, which can differ by a maximum current in main electric lines/phases, supply voltage (depends on customer's country), a number of welding robots, type of welding process and so on. It means that this exactly suggested energy measurement system in chapter 7.1 cannot be applied in every welding cell. On the other hand, Siemens and Festo components are used for every welding cell (program for PLC will not change), but what can differ is voltage and current at the input. For example, if the welding cell is constructed for a factory in Mexico or USA, then the input voltage is 480V AC and ET AI energy meter cannot be connected directly. Thus this, can maximum input current differ too and current transformer can mismatch.

Welding cell which was used for testing of energy measurement system is shown in the following figure:
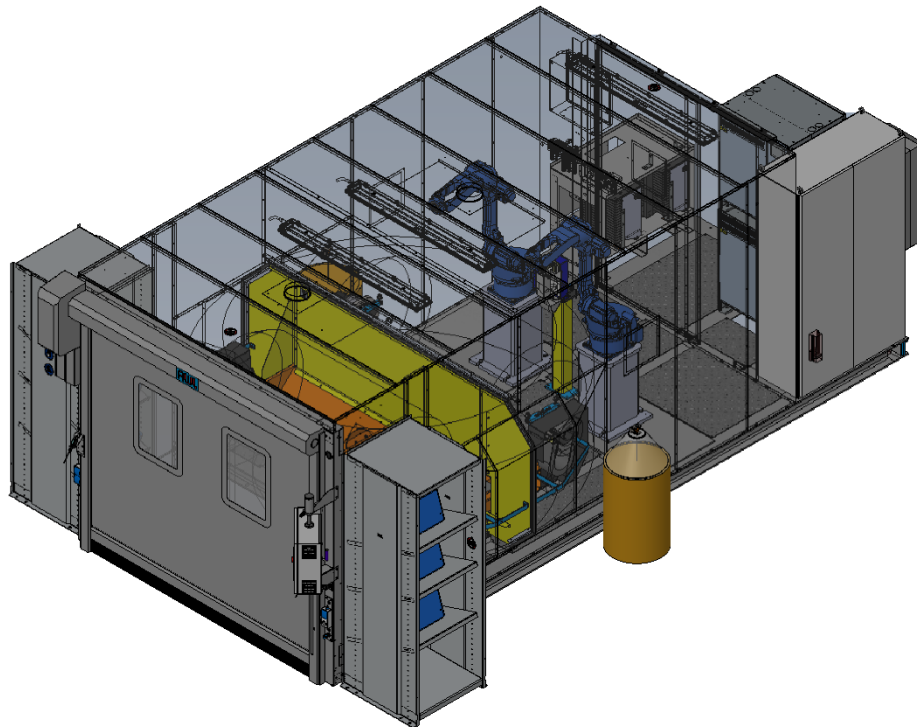

Figure 33: Welding cell used for testing of energy measurement system.

Festo flow meter is placed into the block, between other Festo sensors which are placed on the back side of the welding cell (shown in figure 34) and all electric components are placed in the main switchboard (shown in figure 35).
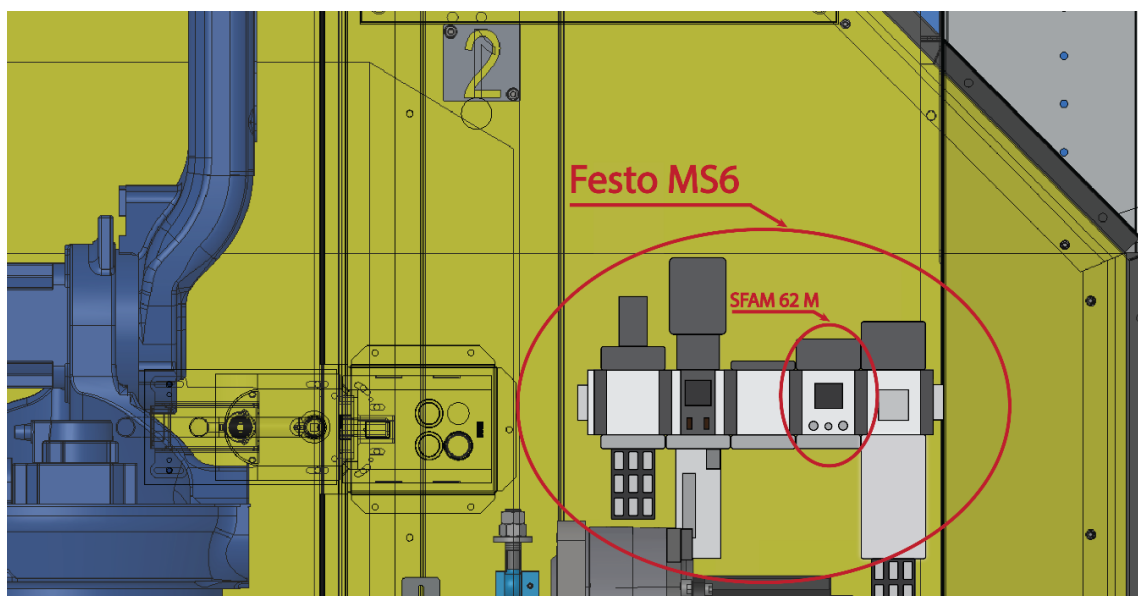

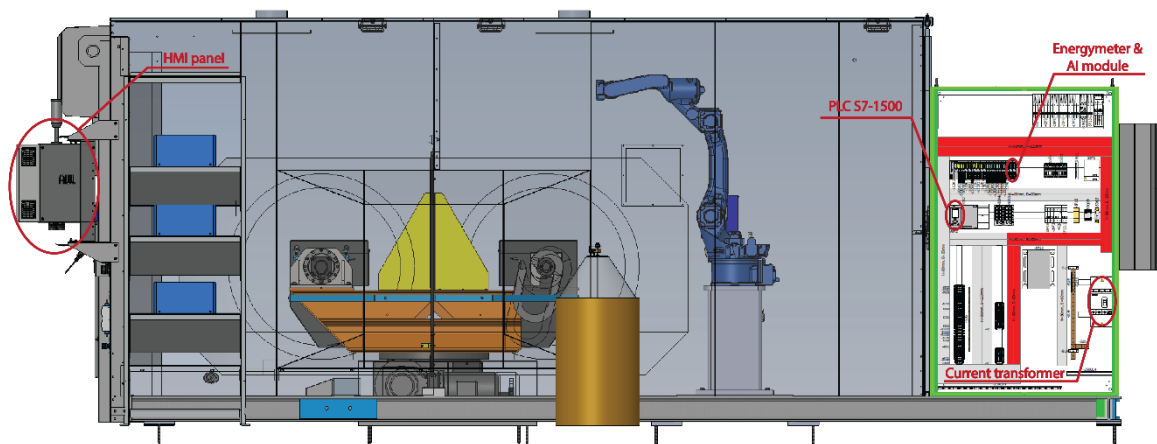Figure 34: Transparent back side view of the used welding cell with Festo flow meter.

Figure 35: Transparent side view of the used welding cell with Siemens components.

In figure 35 are described main components used for measuring of electric energy and the following visualization on HMI panel.

7.3 External PLC for testing purposes

Because welding cells have an own program which must not be modified (because of the modification the machine can be damaged) was used test PLC for programming. Test PLC (SIMATIC S7-1500 – CPU 1516F-3 PN/DP) is separated in external switchboard with the own power source (SITOP PSU100C). Because of the same reasons as for PLC was used external ET I/O station (SIMATIC ET200SP) in second external switchboard where were also placed testing meters. For this purpose was used Festo SFAM 62 T flow meter which differs from proposed SFAM 62 M just in mounting principle and has a stabilizing pipe.
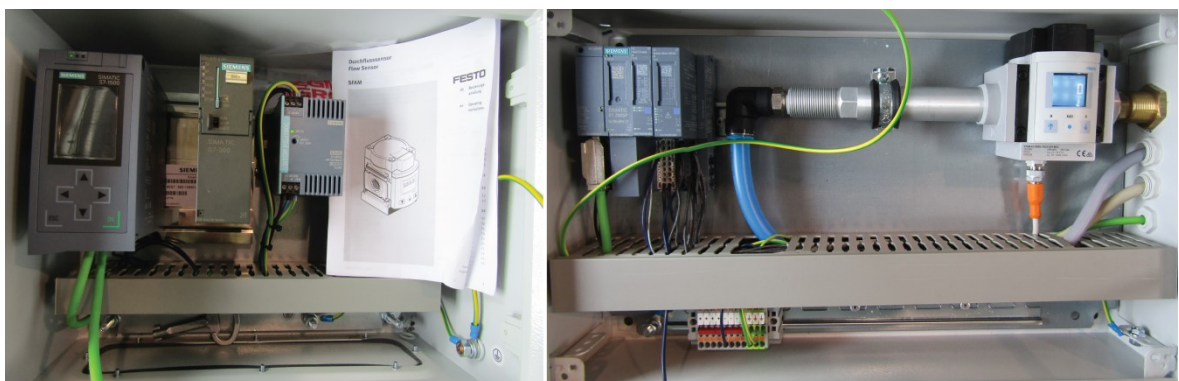
Figure 36: External switchboards with test PLC, energy meter and flow meter.

8 DEVICES CONFIGURATION AND PROGRAM DESCRIPTION

In this chapter is described a process, step by step how and what was necessary to configure, program and problems related to it. Both configuration and programming were done in Siemens TIA portal V13 SP1 (including STEP 7 Professional and WinCC Advanced) but first had to be created test a project for the test program.
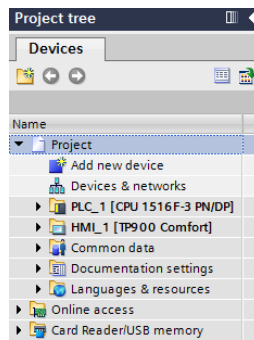

Figure 37: Project tree.

In tab "Devices & networks" are connections between devices and their following configuration. In other two folders (PLC_1 and HMI_1) are programs for PLC and HMI panel including used databases.

8.1 Configuration of devices

After creation of test project were added required devices which were connected by PROFIBUS line. Here are necessary PLC, ET I/O station with modules and HMI panel. After connection of the selected devices was assigned a different IP address to each device in the project and in PLC was configured correct date and time. All other options were preset (Web server communication, max cycle time…) but can be changed in case of need.
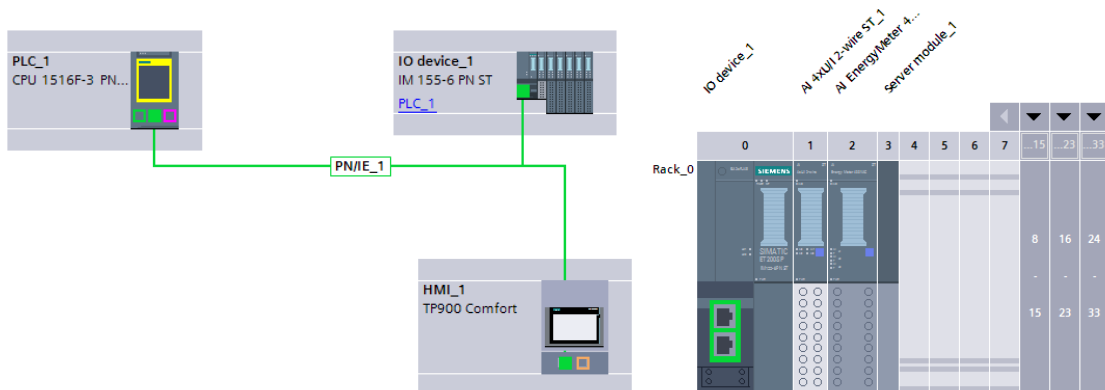

Figure 38: Network view on used devices and device view at ET I/O station.

After that was necessary to configure AI energy meter. It includes line frequency, connection type and user data variant, because energy meter can send different values dependent on the chosen variant. In this case was required to obtain basic values (voltage, current, power factors and frequency). From this basic values can be calculated any power, energy consumption or energy consumption cost. In inputs tab was configured ratio between primary and secondary current and time tolerance for overcurrent. In this case is advantageous this option, because the CPU of PLC is automatically recalculating the secondary current to the primary (real current). Configuration of AI energy meter with user data variants is shown in the following figure.

Figure 39: Configuration menu of AI energy meter.

8.2 Program description

As was mentioned before, whole test program consists of two sections. In first sections are all tags (variables), function blocks and databases which are used by PLC for numerical, logical and other operations. The second section consists mainly of screens and visualization components for HMI panel and basically, there are no scripts because of the idea, in this case, is "do not mix two different program architecture" (PLC scripts are programmed in STEP 7 and HMI scripts are programmed in WinCC). Due to this differences is described each section separately (this chapter is purely about PLC test program).

First of all had to be defined global tags of measured values from measuring devices, which were send in specific data type and have a specific address. In this case, the value of actual flow (in *l/min*) is in word data type – 2 Bytes. From energy meter the values of

current and voltage are unsigned integer data type – 2 Bytes and power factor values are unsigned short integer – 1 Byte. All PLC Tags are shown in the following picture.

		Name	Data type	Address
		MeasValues tag Table PLC		
1		Clock_Byte	Byte	%MB9
2		Clock_10Hz	Bool	%M9.0
3		Clock_5Hz	Bool	%M9.1
4		Clock_2.5Hz	Bool	%M9.2
5		Clock_2Hz	Bool	%M9.3
6		Clock_1.25Hz	Bool	%M9.4
7		Clock_1Hz	Bool	%M9.5
8		Clock_0.625Hz	Bool	%M9.6
9		Clock_0.5Hz	Bool	%M9.7
10		wFlowAnalog	Word	%IW0
11		uiCurrentL1	UInt	%IW10
12		uiCurrentL2	UInt	%IW12
13		uiCurrentL3	UInt	%IW14
14		uiVoltageL1L2	UInt	%IW22
15		uiVoltageL2L3	UInt	%IW24
16		uiVoltageL3L1	UInt	%IW26
17		uiFrequency	UInt	%IW38
18		usiPowerFactorL1	USInt	%IB28
19		usiPowerFactorL2	USInt	%IB29
20		usiPowerFactorL3	USInt	%IB30
21		usiTotalPowerFactor	USInt	%IB31
22		uiVoltageL1	UInt	%IW16
23		uiVoltageL2	UInt	%IW18
24		uiVoltageL3	UInt	%IW20

Figure 40: PLC tag table.

The structure of the test program consists of three FBD function block inserted in main FBD organization block with "program cycle" option. Those three FBD function blocks (namely: fbCalculateTotalEnergyAndPriceEnergy, fbMainFlow and fbMainEnergy with assigned data blocks db fbCalculateTotalEnergyAndPriceEnergy, dbfbMainFlow and dbfbMainEnergy for saving data) are shown in the following figure.

```
▼ 🗂 Program blocks
    📄 Add new block
    🔹 Main [OB1]
    ▼ 🗂 EnergyConsumption
        🔹 fbCalculateTotalEnergyAndPriceEnergy [FB20]
        🔹 fbMainElectricEnergy [FB10]
        🔹 fbMainFlowEnergy [FB3]
        📄 dbfbCalculateTotalEnergyAndPriceEnergy [DB6]
        📄 dbfbMainElectricEnergy [DB5]
        📄 dbfbMainFlowEnergy [DB2]
    ▶ 🗂 EnergyMeasurement
    ▶ 🗂 FlowMeasurement
    ▶ 🗂 TotalEnergyCalculation
```
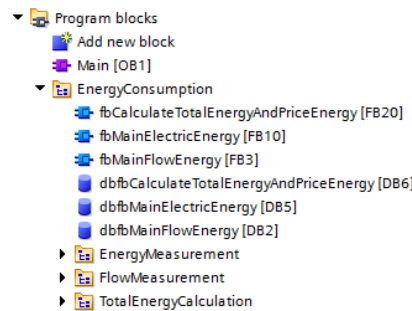
Figure 41: Main organization block.

All the three FBD function blocks consists of SCL function blocks, where calculated energy values are stored in certain data blocks. The principle is following. Data which are received are selected and stored by PLC memory in certain time. In this case, are processed only received data from the flow meter and energy meter in the period of 1s. These data are considered as actual and are further stored in the 60-second array in the database of the certain data block. When is reached the time horizon of 60 seconds, the values in the array

are averaged and they are further overwritten by new values. The 60 second averaged value gives the 1-minute value which is written into the 60-minute array. This algorithm is applied for all other time values which are included in structured data type – DTL. DTL data type consists of time values: *ns, s, min, hour, month, and year*. The whole algorithm of calculation and storing values is described in the following figure (including stored values and their data type).
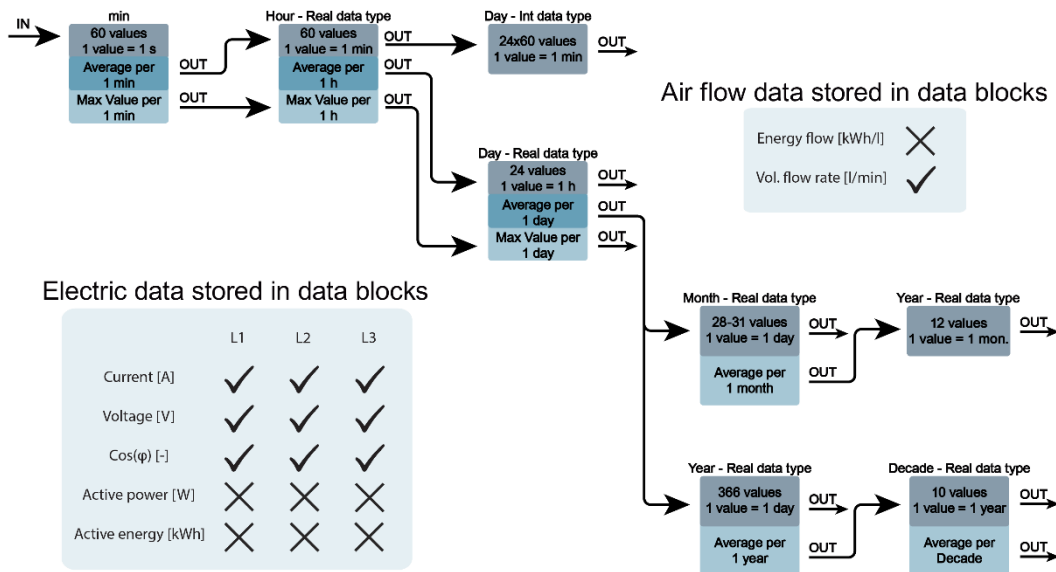

Figure 42: Data flow and data store diagram.

Since very beginning was a highly discussed topic of memory space consumption because the original program needs certain memory and implemented energy measurement system should not consume too much space and should not significantly slow CPU of PLC. In addition, there must be still space for add-ons or improvement of the whole program. Due to this are stored only basic values (currents, voltages, power factors and volumetric flow rate of compressed air). Another topic to discuss is what data types should be used for stored and calculated data. It is for deeper research for which was not time. Data can be stored in integers or short integers and then can be recalculated to their original value or can be stored in real data type for higher accuracy. At the end, the structure ended in form like this, where the PLC cycle takes at maximum 3ms and the stored data consumes up to 3% of PLC internal memory.

In total there are 16 SCL function blocks (fb) for calculation and storing measured and calculated data (8 fb for flow values and 8 fb for electric values). A first function block

is used for conversion and changing of a data type of the received data (these values are considered as actual values). The second data block is for selecting and calculating minute values, third for hour values, fourth for day values, fifth for month values, sixth for year values, seventh for decade values and eighth for calculating of power, energy, and energy cost values. In following, pages are described only SCL function blocks with conversion, energy price, minute and decade algorithm because the data storage algorithm is in other blocks almost same (month blocks have some additional commands because the months have not fixed day count).

8.2.1 Analog flow values conversion to digital values

During the conversion of the measured values to the real ones which are in l/min were found several problems. The Festo flow meter is sending small value which is considered as noise and is approximately 147. After this when was known that 0 l/min=147 was necessary to find out what analog output number for 5000 l/min is. Because of that were measured the static characteristic of the flow meter, values of air flow were read from the display of the flow meter when PLC received unknown digital numbers/values.
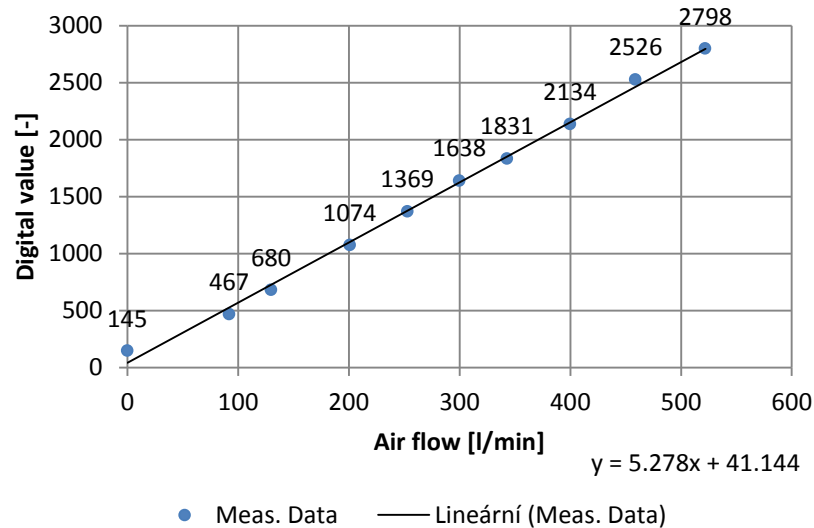
Figure 43: Static characteristic of SFAF 62 T.

During the measurement of static characteristic was found that the flow rate of compressed air can be at maximum $V = 530$ l/min and chosen flow meter to have too wide measurement range and low accuracy in small flow rate. On the other hand, in welding cells is used a system based on bool logic (closed valve = 0 air flow, opened valve = maximum air flow). Due to this is considered that the measured air flow will be always at maximum and for

these flow rate of 530 l/min is flow meter relatively accurate. The maximum digital value for 5000 l/min can be calculated from the computed linear equation:

$$y = 5.278x + 41.414 = 5.278 \cdot 5000 + 41.414 \approx 26430 \tag{67}$$

From known constants is now possible to convert received digital value to the actual flow rate by the following equation.

$$\dot{V}_{actual} = (AI - 147) \cdot \frac{5000}{26430} \tag{68}$$

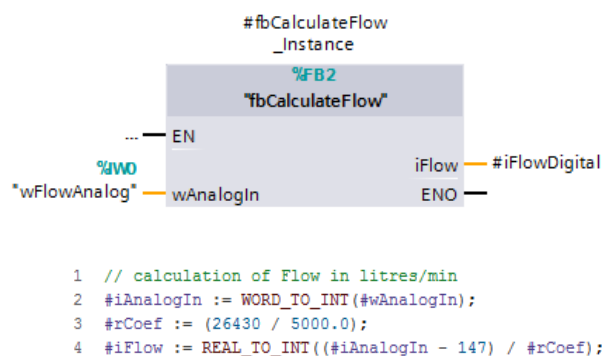This equation is represented by short SCL script in SCL block in the following figure:


```
1  // calculation of Flow in litres/min
2  #iAnalogIn := WORD_TO_INT(#wAnalogIn);
3  #rCoef := (26430 / 5000.0);
4  #iFlow := REAL_TO_INT((#iAnalogIn - 147) / #rCoef);
```

Figure 44: SCL block with the script for analog values conversion to flow values.

8.2.2 Analog energy values conversion to digital values

The conversion of energy values was not too much complicated. Basically were only changed data types and physical quantity. Current is converted from mA to A, Voltage from 0.01V to V and power factor from 100 [-] to 1 [-].

```
1  //Convertion of Uint miliamperes to int Amperes for each line
2  #iCurrentL1 := UINT_TO_INT(#uiCurrentL1) / 1000;
3  #iCurrentL2 := UINT_TO_INT(#uiCurrentL2) / 1000;
4  #iCurrentL3 := UINT_TO_INT(#uiCurrentL3) / 1000;
5
6  //Convertion of Uint 0.01V to int Volts for each L-N and L-L conection
7      //L-N connection
8      #iVoltageL1 := UINT_TO_INT(#uiVoltageL1) / 100;
9      #iVoltageL2 := UINT_TO_INT(#uiVoltageL2) / 100;
10     #iVoltageL3 := UINT_TO_INT(#uiVoltageL3) / 100;
11
12     //L-L connection
13     #uiDummyVL1L2 := (#uiVoltageL1L2) / 100;
14     #iVoltageL1L2 := UINT_TO_INT(#uiDummyVL1L2);
15     #uiDummyVL2L3 := (#uiVoltageL2L3) / 100;
16     #iVoltageL2L3 := UINT_TO_INT(#uiDummyVL2L3);
17     #uiDummyVL3L1 := (#uiVoltageL3L1) / 100;
18     #iVoltageL3L1 := UINT_TO_INT(#uiDummyVL3L1);
19
20 //Convertion of USint power factor to int power factor - cos(fi)
21     #rPowerFactorL1 := USINT_TO_REAL(#usiPowerFactorL1) / 100;
22     #rPowerFactorL2 := USINT_TO_REAL(#usiPowerFactorL2) / 100;
23     #rPowerFactorL3 := USINT_TO_REAL(#usiPowerFactorL3) / 100;
```

Figure 45: SCL script for analog energy values conversion to digital values.

8.2.3 Data storage script

For example was used average minute flow script. As was mentioned before only received data from flow meter in the period of 1s are further processed due to the tag *#iSecond* which is incrementing by 1 each second till the new minute starts. This incrementation is dependent on the structured data type DTL.

```
1  #idummy := RD_SYS_T(#actual_time);
2  //setting the actual second in time
3  #iSecond := #actual_time.SECOND;
```

Figure 46: Actual second script part.

Next part of the script is focused on gaining the starting second because of measurement starting time and the last second (in this case the last second is not important but it is important in the script for month values where the month does not have fixed day count). These tags are used further for calculating the correct average minute value and for correct data storing.

```
5  //find start time of writing values to min array
6  if #MinSecond >= #iSecond then
7      #MinSecond := #iSecond;
8  else
9      #MinSecond := #MinSecond;
10 end_if;
11 //find end time of writing values to min array
12 if #MaxSecond <= #iSecond then
13      #MaxSecond := #iSecond;
14 end_if;
```

Figure 47: Start time and end time script part.

Insertion of measured data to the array will proceed only in the case when the actual second will increment/change because the script can cycle thousands of times per second and the array cell would be overwritten each cycle which is highly inefficient.

```
16 if #iSecond > #tLastSEC then
17      "dbMeasuredFlow".MeasValuesInM[#iSecond] := #iFlow;
18      #tLastSEC := #iSecond;
19      if #iSecond >= 59 then
20          #tLastSEC := -1;
21      end_if;
22 end_if;
```

Figure 48: Values insertion into database array.

In the minute, hour and day scripts are also calculated maximum values as bonus information. In other scripts (month, year, decade) are not calculated because is assumed that the maximum values should not much differ in bigger time horizon. The principle is as

follows. If the actual value is bigger than the past maximum value, then the maximum value is overwritten otherwise nothing change.

```
25 ⊟if #iMaxFlowPerMin <= #iFlow then
26         #iMaxFlowPerMin := #iFlow;
27  end_if;
```

Figure 49: Max value calculation.

In last part of the script is calculated average and the value of the previous average and maximum are set to zero.

```
30 ⊟if #iSecond = 0 then
31         #bCalculated := false;
32  end_if;
33  //resseting max and average value of flow, calculating average of flow in minute
34 ⊟if #iSecond >= 59 and not #bCalculated then
35         #bCalculated := true;
36         #iMaxFlowPerMin := 0;
37         #iAverageFlowPM := 0;//need to reset cause it has value from previous cycle
38
39 ⊟      for #j := #MinSecond to #MaxSecond by 1 do
40             #iAverageFlowPM := #iAverageFlowPM + "dbMeasuredFlow".MeasValuesInM[#j];
41         end_for;
42         #iAverageFlowPM := #iAverageFlowPM / (1+#MaxSecond - #MinSecond);
43
44         #MinSecond := 60;
45         #MaxSecond := 0;
46  end_if;
```

Figure 50: calculation of average value.

In row 30, if the new minute starts the tag #bCalculated is set as false. Then in row 34, if actual second (#iSecond) in time is higher or equal to 59 (60s) and the tag #bCalculated is false then the tag #bCalculated is set as true (in next nanosecond cannot be calculated average value, otherwise in the next nanosecond is tag #MaxSecond set to 0 and the average value would be calculated with result equaled to 0 – row 45). In following rows are reset tags #iMaxFlowPerMin and #iAverageFlowPM. In "for" cycle is calculated a sum of stored values from the minute array of the database (TIA portal does not have function/command for the sum). In row 42 is calculated an average value, where the number of seconds is given by the difference of last second in the minute and starting second in the minute (if the measurement starts at 35 seconds, then the starting second - #MinSecond = 35. In the minute script it does not have much weight, but in month script it is noticeable). In the next second when #iSecond = 0 is #bCalculated set as 0. The average value can be written as the well-known equation:

$$Aver.Value = \frac{1}{1 + s_{max} - s_{min}} \sum_{j=s_{min}}^{s_{max}} array(j) \qquad (69)$$

Because of structured data type DTL, which is working in maximum with years is necessary to use a different algorithm for decade script.

```
13 ⊟if (#iYear - #iPrevYear) >= 1 then
14     //inserted measured values of year into decade arra
15     "dbMeasuredFlow".MeasValuesinDeByY[#i] := #rAverageFlowPerYear;
16     #i := #i + 1;
17
18 ⊟    if #i > 9 then
19         //reset of average flow after decade (retain value from previous decade)
20         //and setting the start time for 3000 for initial condition
21         #i:=0;
22         #rAverageFlowPDec := 0;
23         #dStartTime := 3000;
24
25         //calculating the average flow after decade
26 ⊟        for #j := 0 to 9 by 1 do
27             #rAverageFlowPDec := #rAverageFlowPDec + "dbMeasuredFlow".MeasValuesinDeByY[#j];
28         end_for;
29         #rAverageFlowPDec := #rAverageFlowPDec / 10;
30     end_if;
31
32     #iPrevYear := #iYear;
33 end_if;
```

Figure 51: Average value calculation in decade script.

The condition on the 13th row is met only in the case when the value of actual year minus previous year is bigger or equal to 1 otherwise the value of actual year minus previous year = 0 (next cycle which is in next millisecond). If the condition is true then can be written an average value of the year to the decade array and the tag for the previous year is set to the actual year (the condition in row 13 will not meet for another year). Condition on the 18th row is met when incrementing #i < 9, after that is increment #i reset, starting the year is set to 3000 and the average value is reset too. In following rows is calculated average decade value by the same algorithm as in other scripts.

8.2.4 Energy consumption and its cost calculation

As in previous topics, the energy consumption algorithm will differ for compressed air flow energy (is necessary calculate how much energy consumers compressor's motor) and for electric energy. The energy cost algorithm for the compressed air is shown in following equations:

$$E_V \left[\frac{kWs}{l}\right] = \frac{P_{motor}[kW]}{\dot{V}_{comp.max}\left[\frac{m^3}{min}\right] \cdot \frac{1000}{60}} \qquad (70)$$

Then the consumed energy (*FE*) can be calculated (here are for example calculated actual, minute and hour values of the consumed energy and its cost):

$$FE_{actual} \ [kWs] = \frac{\dot{V}}{60} \left[\frac{l}{s}\right] \cdot E_V \left[\frac{kWs}{l}\right] \cdot 1s \tag{71}$$

$$FE_{min} \ [kWs] = \frac{\dot{V}}{60} \left[\frac{l}{s}\right] \cdot E_V \left[\frac{kWs}{l}\right] \cdot 60s \tag{72}$$

$$FE_{hour} \ [kWh] = \frac{\dot{V}}{60} \left[\frac{l}{s}\right] \cdot E_V \left[\frac{kWs}{l}\right] \cdot \frac{3600s}{3600} \tag{73}$$

The cost of the compressed air flow energy (CFE) can be calculated from previous equations.

$$CFE_{actual}[Eur] = E_{actual} \ [kWs] \cdot Price \left[\frac{Eur}{kWh}\right] \cdot \frac{1}{3600} \tag{74}$$

$$CFE_{min}[Eur] = E_{min} \ [kWs] \cdot Price \left[\frac{Eur}{kWh}\right] \cdot \frac{1}{3600} \tag{75}$$

$$CFE_{hour}[Eur] = E_{hour} \ [kWh] \cdot Price \left[\frac{Eur}{kWh}\right] \tag{76}$$

For electric energy (*EE*) are calculated total active power (*P*) and total reactive power (*Q*) based on equation (28), where the equation for reactive power is modified ($cos\varphi \Rightarrow sin\varphi$). The equation for the price of active energy (*CEE*) is (for example calculated actual, minute and hour values of the active energy cost):

$$CEE_{actual}[Eur] = \frac{EE \ [Ws]}{3600000} \cdot Price \left[\frac{Eur}{kWh}\right] \tag{77}$$

$$CEE_{min}[Eur] = \frac{EE \ [Ws] \cdot 60s}{3600000} \cdot Price \left[\frac{Eur}{kWh}\right] \tag{78}$$

$$CEE_{hour}[Eur] = \frac{EE \ [Wh]}{1000} \cdot Price \left[\frac{Eur}{kWh}\right] \tag{79}$$

Then the total energy and its cost are calculated by simple summation, where index *i* represents given time sequence (*s, min, hour, day, month, year, and decade*).

$$E_i \ [kWh] = FE_i + EE_i \tag{80}$$

$$C_i \ [Eur] = CFE_i + CEE_i \tag{81}$$

8.3 Integration of test program into cell program

The idea of integration of test program is since the very beginning almost given. Simply add/import the created function blocks into cell program and HMI screens to between the others screens. There must be met condition with tags and the addresses of modules because their global addresses will change. Because of that were used only static intern tags (not global tags) what is

highly redundant but it ensures that tags of test program will not overwrite the cell program tags. The network view of the configured devices looks similar to one in the following figure.
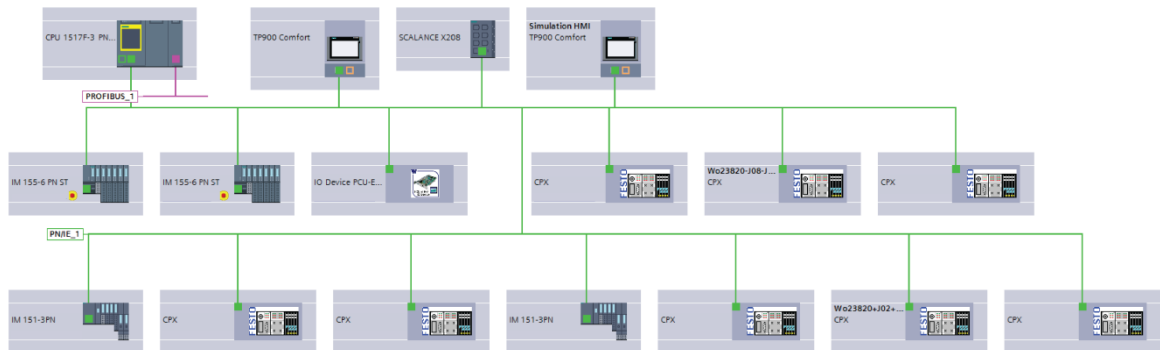
Figure 52: Network view of the welding cell.

The AI module and energy meter can be then easily integrated to one of the ET modules IM 155-6 PN ST.

8.4 HMI visualization and its integration

HMI visualization is made in accordance with a visual identity of AWL-Techniek and visual components which were made should be integrated into the HMI visualization of the welding cell. For visualization of the measured data is necessary to import PLC tags into HMI tag table because the PLC database is not shared. 198 Tags were created for test HMI visualization. HMI TP900 Comfort panel can work with up to 512 tags = 12 MB HMI memory (all tags are exported into appendix 3). This number of tags is final but can be reduced in the future if there will be need of it. All visualization components (screens) should be part of main screen "Energy consumption" located in the cell HMI main menu (shown in the following figure).
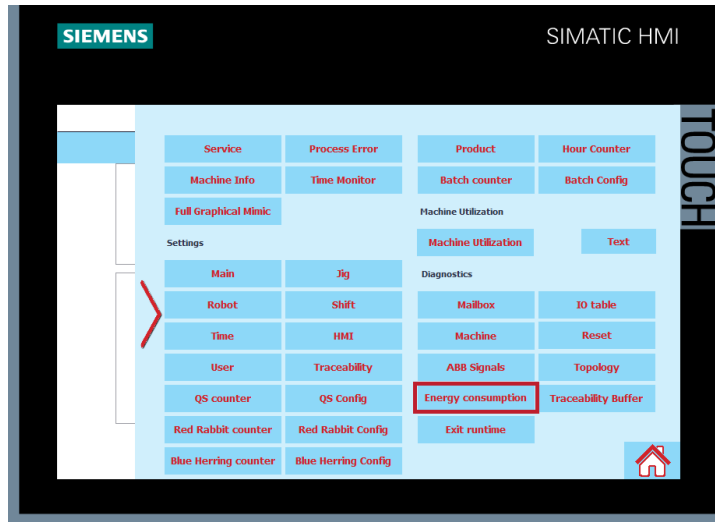
Figure 53: Cell HMI main menu with integrated energy consumption visualization.
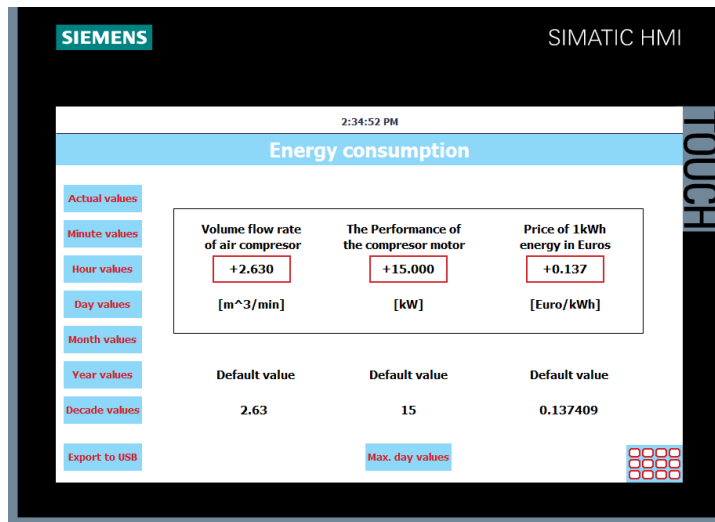
Figure 54: Main screen of energy consumption menu.

In energy consumption root screen, are located boxes which are giving an option to input own values for calculation of energy consumption. Those values are volume flow rate of an air compressor ($\dot{V}_{comp.max}$ [m^3/min]), the Maximum performance of the electric motor in used compressor (P_{motor}[kW]) and price for electric energy $\left(Price\left[\frac{eur}{kWh}\right]\right)$. From this root screen, links are in form of buttons to other screens with tables (actual, minute, hour, day, month, year and decade tables) and to the screen with a table that contains the maximum day current, voltage, and air flow values.
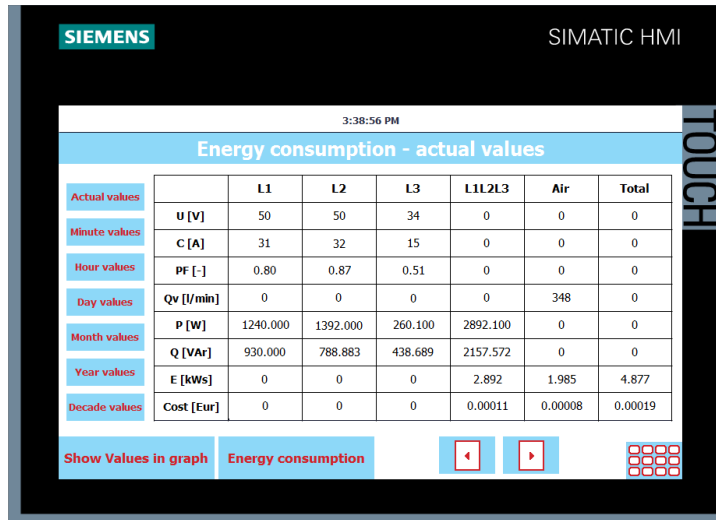
Figure 55: Table screen with measured and calculated values.
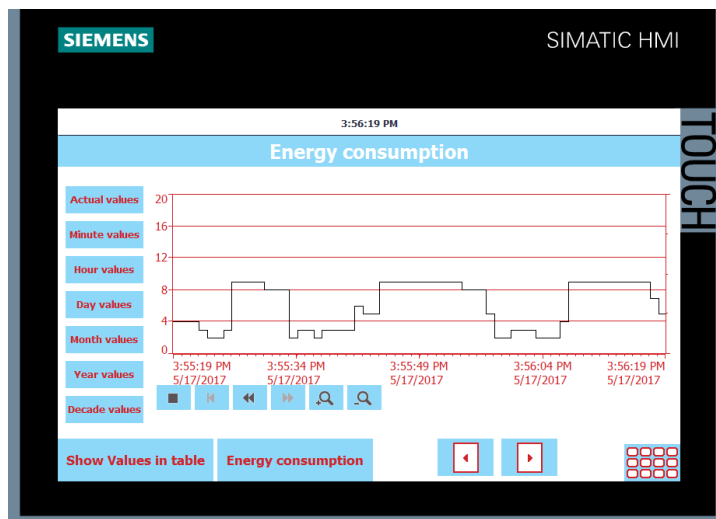
Figure 56: Graph screen with measured and calculated values.

The switching between graph screen and table screen is ensured by button "show values in table/graph". There is also an option for a jump back to the root screen (Energy consumption button). For switching between neighbors (graphs/tables) are used left and right arrow buttons. In the bottom right corner is located button for the main menu. For a view of the maximum day values, is necessary to get back to the energy consumption root screen (Maximum day values are only visualized in the table). Button Export to USB is for exporting measured integer values to USB flash drive, which is connected with HMI panel. This solution is more problematic because the USB port is from the back side of the HMI panel and not all customers must have access to it.

9 PRACTICAL VERIFICATION OF THE ENERGY MEASURING SYSTEM

For the practical verification were used knowledge, devices, and program which are described in previous chapters. For obtaining real data was used welding cell, constructed for Johnson Controls which is shown in figure 33.

The flowmeter was connected to the compressed air distribution through the air pistol. With the pistol can be controlled air flow which was used during the first measurements. The correctness of calculated values of flow was given by comparing of calculated values with values on the flow meter's display.

The output wires from the current transformer were connected to the socket of energy meter located in the ET200SP I/O station with accompany of voltage wires through terminal blocks which are shown in the following figure.

Figure 57: Electric connection of the energy meter to
the welding cell distribution.

The shown connection was used only for verification because the welding cell was before export. In any case around the main switchboard was created a safe zone with the distance of 1m. The connection and function have been verified during the teaching process when the robots are moving on wanted trajectories which usually take few hours.

The algorithms for storing of measured data and their further calculations were verified continuously. As first, algorithms and programs were tested for compressed air which final version was applied for electricity measurement.

10 DATA ANALYSIS

In this chapter is outlined reason why measurements of energy in such a case are made. Usually, measured data of energy consumption are used for its cost calculation and so for further economic analysis. There is also an ecological aspect which is in past few years highly discussed topic and is certainly among priorities of the modern company. It is closely related to so-called "Energy management system" which will be briefly described in next chapter.

10.1 Energy management system

An energy management system is a system composed of computer-aided tools for monitoring, controlling and optimizing the performance of the machines/buildings or other devices with the purpose to reduce their energy consumption. There are several voluntary regulations covered by ISO norms, ASHRAE/IES standards, ANSI/MSE standards and many others standards which are trying to help reduce the energy consumption in the industrial sector. More precisely ASHRAE/IES 2016 – energy efficiency standard (more focused on energy consumption of buildings), ANSI/MSE 2000 – US energy management standard (plan, do, check, act) and worldwide norm ISO 50001 – energy management system which replaced previous norm EN 16001 and is closely related with ISO 9001 - quality management system. ISO 50001 generally covers all today's used/proposed standards by other institutes or organizations. This norm should help establish energy management in industrial, commercial, institutional or governmental facilities. Based on sources is estimated that the norm could influence up to 60% of the world's energy use. [24]

10.2 Economic aspect of energy measurement

For industrial welding, companies are information about energy consumption highly important, because as it is known welding process is demanding for electricity (how much? It depends on the type of welding process and standard). If the company would like to expand its production, then the price of the electricity for industrial consumers will play a huge role in company's decision. Next figure shows electricity prices for industrial consumers for the first half of 2016 in *Euro/kWh*.
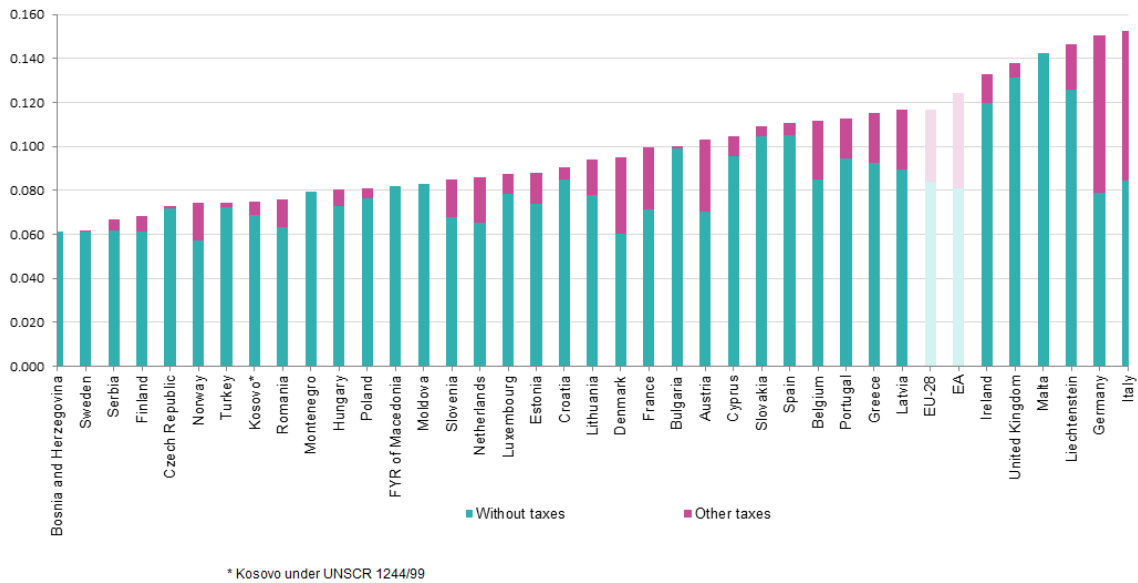
Figure 58: Electricity price for industrial consumers for European countries, 2016. [25]

In figure 58 are not included world countries but for comparing the average price in the USA that time was around 0.05 Euro without taxes, 0.055 Euro in Russia, 0.06 Euro in Canada without taxes [26], 0.027 Euro in Mexico [27]. A little bit lower price of electricity are then in India and China.

For compare, let's say that welding machine is connected to the electricity with unbalanced load but without THD. The measured average year (month has 30 days) values of currents, voltages and power factors are: $U_1 = U_2 = U_3 = 230V, I_1 = I_2 = I_3 = 19A, \cos \varphi_1 = 0.6, cos\varphi_2 = -0.3, cos\varphi_3 = 0.7$ then can be calculated average energy consumption over the year – based on the equation (23).

$$P = UI[cos\varphi_1 + \cos \varphi_2 + cos\varphi_3] = 4370 \ W \qquad (82)$$

$$E = P \cdot time = 51508.224MWs = 37.7568 \ MWh \qquad (83)$$

From the equation (83) can be calculated the cost of electric energy depending on the country. For example, six different countries are shown in the following table (based on equation 84).

$$C = E \cdot Price \qquad (84)$$

For further calculation were selected Poland, Mexico, USA, Germany, Russia and Spain because of different energy pricing, geography, and standard of living.

Table 2: Energy cost comparison of welding cell in

different countries.

Country	Price [EUR/kWh]	Cost [EUR]
Poland	0.080	3020.544
Germany	0.150	5663.520
Spain	0.140	5285.952
Russia	0.055	2076.624
USA	0.050	1887.840
Mexico	0.027	1019.434

The calculated operating cost of electricity can mismatch and there is no guarantee on their correctness (several sources, 1-year-old statistics). The purpose of table 2 is to show how much the energy costs can differ in each country. Usually the costs for a company are much higher because in these examples the values are calculated only for one welding cell, and usually, there is several or many of them (depends on the size of company).

On the other hand cost of electricity is not the only one factor. There are other factors like quality of electric energy distribution which includes THD or how balanced the electric grid is. The quality is also affected by weather (big temperature differences). Of course should be mentioned living standard in the country, law system, taxes, logistics and human resources which are related to the education system.

CONCLUSION

Since the beginning, it was clear how the measurement system should look and how it should be integrated into existing systems because the welding cell consists exclusively of Siemens and Festo automated components. Hence their proposed measurement devices were focused on first and then at the end were bought and applied. Problems occurred during the configuration when it was found that inappropriate flow meters were chosen because they had too wide of a measurement range (50-5000 l/min), but for welding cells, the flow meter with the smallest range (10-1000 l/min) is required. Because of this, the measured values of air flow were not accurate, and for further application, the flow meter should be changed. This issue occurred mainly because the plans and other documents did not specify the maximum air flow in the machine and pipes, and the "middle strong" version of the flow meter was chosen.

The next topic discussed was PLC memory space consumption, which is affected by the amount of stored data and data type. This stored data should take as little space as possible because there must be space for rest of the machine program and further add-ons or improvements. In the end, the test program which should be implemented took 10% of PLC internal memory where PLC cycle time took at maximum 3 *ms*, which can be defined as a satisfying result.

The whole program consists of two sections. In the first section are all tags, function blocks and databases used by PLC and in the second section are tags, visualization and possible scripts for HMI panel. This separation caused several problems because scripts for PLC are programmed in STEP 7 and possible scripts for HMI in the programming language of WinCC, which is totally different. During the visualization, there were problems such as WinCC cannot display a static graph, cannot export values of real data types or bits.

At the very end of this thesis, options are outlined for further analysis of measured data. In one short example, the annual cost of energy in accordance to certain countries is shown. From the proposal perspective, it can be said that this measuring system should be attractive for AWL customers. The measured data of energy consumption can help the customer to optimize his production, and the cost related to the added measuring devices is less than 800 Euro, which is more than tempting.

BIBLIOGRAPHY

[1] DRECHSLER, Richard. *Měření vyhodnocení a kvalita odběru elektrické energie v provozu tyristorových zařízení*. 1. Praha: SNTL, 1982, 134 s.

[2] *Vyšší harmonické a jejich působení na síť* [online]: Praha: FCC Public, 2008 [cit. 2017-05-15]. Available from: http://www.odbornecasopisy.cz/elektro/casopis/tema/vyssi-harmonicke-a-jejich-pusobeni-na-sit--11949

[3] *Harmonic filter AHF* [online]: Boston: Danfoss, 2008 [cit. 2017-05-15]. Available from: http://files.danfoss.com/documents/PE/doc_MG80C302.pdf

[4] *Bandstop Filters for microwave filter design* [online]. TaiPei: NTU, 2011 [cit. 2017-05-15]. Available from: http://ntuemc.tw/upload/file/20110503143218e921b.pdf

[5] *Active filter design and specification* [online]. Knoxville: Electrotec, 2005 [cit. 2017-05-15]. Available from: http://www.pqmonitoring.com/papers/Harmonic%20Distortion%20Issues/active%20filter.PDF

[6] *Practical active filter design by means* [online]. Sunnyvale: Linkedin 2015 [cit. 2017-05-15]. Available from: https://www.slideshare.net/SachinMehta12/practical-active-filter-design-50621356

[7] *Harmonics generation, propagation and purging techniques in non-linear loads* [online]. New York: Intech, 2011 [cit. 2017-05-15]. Available from: http://cdn.intechopen.com/pdfs-wm/43901.pdf

[8] *Nine level cascaded multilevel inverter simulation* [online]. Delhi: ABiswal 2013 [cit. 2017-05-15]. Available from: http://www.123mylist.com/2013/04/9-level-cascaded-multilevel-inverter.html

[9] *Měřící modul pro pracoviště aktivního harmonického filtru* [online]. Praha: ČVUT, 2015 [cit. 2017-05-15]. Available from: https://dspace.cvut.cz/bitstream/handle/10467/61912/F3-BP-2015-Sevcik-Jan-Merici_%20modul_pro_pracoviste_aktivniho_harmonickeho_filtru.pdf?sequence=1

[10] *Biot-Savart law and its application* [online]. Bengaluru: BYJUS, 2017 [cit. 2017-05-15]. Available from: http://ictwiki.iitk.ernet.in/wiki/index.php/Biot_Savart%27s_Law_and_its_applications

[11] Electrical and Electronics Measurements and Instrumentation: Prithwiraj Purkait, Budhaditya Biswas, Santanu Das, Chiranjib Koley, 2013, ISBN: 978 93 8328 679 9

[12]   Technické prostředky Integrované automatizace, František Hruška, 2012, ISBN: 978 80 7454 234 3

[13]   *Smart metering: cesta od mechanického elektroměru k chytrým sítím* [online]. Brno: VUT 2012 [cit. 2017-05-15]. Available from: http://www.crr.vutbr.cz/system/files/ brozura_10_1212.pdf

[14]   *Real gas and non-hypothetical gasses* [online]. 2017 [cit. 2017-05-15]. Available from: https://en.wikipedia.org/wiki/Real_gas

[15]   *Měření průtoku a výšky hladiny*. Praha: BEN-Technická literatura, 2005, s. 447. ISBN 80-7300-156-X.

[16]   *Applications of the Bernoulli equation* [online]. UK: School of civil engineering 2006 [cit. 2017-05-15]. Available from: http://www.efm.leeds.ac.uk/CIVE/CIVE1400/Section3/ bernoulli-apps.htm

[17]   *ABB electricity meter A43 212-100* [online]. Bern: ABB, 2017 [cit. 2017-05-15]. Available from: http://new.abb.com/products/2CMA170522R1000/active-energy-cl-b

[18]   *Siemens SIMATIC ET200SP AI module* [online]. Berlin: Siemens, 2017 [cit. 2017-05-15]. Available from: https://mall.industry.siemens.com/mall/en/WW/Catalog/Product/6ES7134-6PA01-0BD0

[19]   *METSEPM3250 power meter Schneider electronic* [online]. Le Crueset: Schneider, 2016 [cit. 2017-05-15]. Available from: http://www.schneider-electric.com/en/product /METSEPM3250/pm3250-power-meter---rs485/?range=61274-powerlogic-pm3000-series &node=166377571-products&parent-subcategory-id=4115&parent-category-id=4100

[20]   *Compressed air counter DN15-50, Testo 6441-6444* [online]. Lenzkirch: Testo 2014 [cit. 2017-05-15]. Available from: https://media.testo.com/media/72/3c/26b3460897d1/ Prospekt-testo-110.pdf

[21]   *Aventics Series AF1 flow sensors* [online]. Laatzen: Aventics 2016 [cit. 2017-05-15]. Available from: http://www.aventics.com/pneumatics-catalog/Pdf.cfm?Language=EN&file =en/pdf/PDF_g197167_en.pdf

[22]   *Festo Flow sensors SFAM* [online]. Esslinger am Neckar: Festo 2013 [cit. 2017-05-15]. Available from: https://www.festo.com/cat/en-gb_gb/data/doc_ENGB/PDF/EN/SFAM_EN .PDF

[23]   *Festo Flow sensors SFAM image* [online]. Sleaford: Kiowa 2013 [cit. 2017-05-15]. Available from: http://www.kiowa.co.uk/674-P00065651/SFAM-62-5000L-M-2SA-M12-Festo-Flow-sensor-

[24]   *Energy challenge with ISO 50001* [online]. Geneva: ISO 2011 [cit. 2017-05-15]. Available from: https://www.iso.org/files/live/sites/isoorg/files/archive/pdf/en/iso_50001_energy.pdf

[25]   *Electricity price statistics* [online]. Brussel: Eurostat 2017 [cit. 2017-05-15]. Available from: http://ec.europa.eu/eurostat/statistics-explained/index.php/Electricity_price_statistics

[26]   *International industrial energy prices* [online]. London: GOV, 2017 [cit. 2017-05-15]. Available   from: https://www.gov.uk/government/statistical-data-sets/international-industrial-energy-prices

[27]*Mexican Report* [online]. México City: NERA, 2016 [cit. 2017-05-15]. Available from: http://www.nera.com/content/dam/nera/publications/2016/PUB_Mexican_Electricity_Market_Report_1016_Rev.pdf

LIST OF ABBREVIATIONS

AC   Alternating Current

DC   Direct Current

DHT   Total Harmonic Distortion

PWM   Pulse Width Modulation

IGBT   Insulated Gate Bipolar Transistor

MCU   Micro Controller Unit

RAM   Random Access Memory

CPU   Central Processing Unit

WAN   Wide Area Network

I/O   Input Output

AI   Analog Input

BI   Binary Input

DN   Diameter Nominal

PLC   Programmable Logic Controller

TIA   Totally Integrated Automation

PN/IE   Profinet Network/Industrial Ethernet

FBD   Function Block Diagram Language

SCL   Structured Control Language

FE   Flow Energy $[kWh]$

E_V Energy in Volume $[kWh\,l^{-1}]$

CFE   Cost of Flow Energy

EE   Electric Energy

CEE   Cost of Electric Energy

LIST OF FIGURES

LIST OF TABLES

APPENDICES

P I   Block diagram of the AI energy meter ST

P II   Connection diagram and parameters of the flow meter

P III   Table with a sample of used tags

APPENDIX P I: BLOCK DIAGRAM OF THE AI ENERGY METER ST

①	Microcontroller	UL_n	Voltage connection
②	Backplane bus interface	IL_n	Current connection
③	Analog-to-digital converter (ADC)	N	Neutral conductor
④	Power measurement		
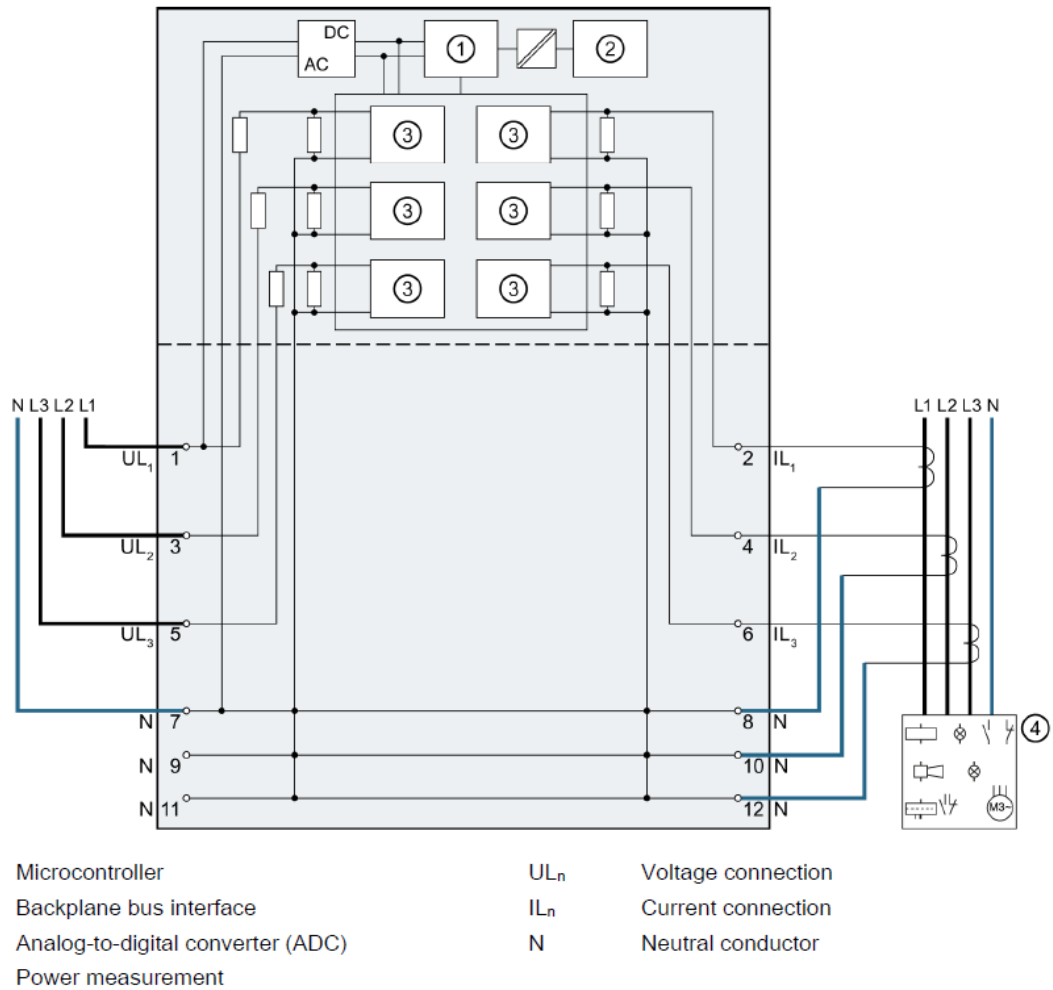
Block Diagram of the AI energy meter ST is taken from "SIMATIC ET 200SP analog input module AI Energy Meter ST Manual".
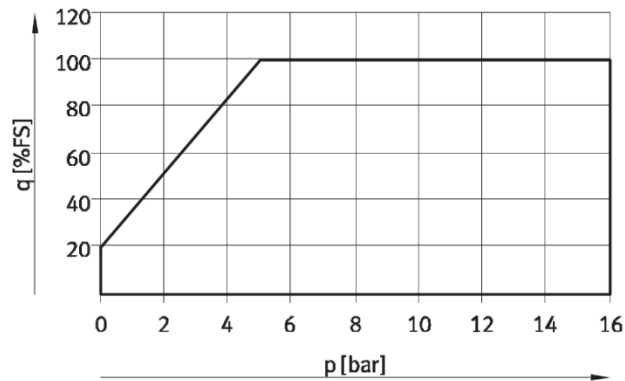
Siemens SIMATIC ET200SP AI Energy Meter ST Manual [online]. Berlin: Siemens, 2014 [cit. 2017-05-15]. Available from: https://cache.industry.siemens.com/dl/files/696/73098696/att_31267/v1/et200sp_ai_energymeter_st_manual_en-US_en-US.pdf

APPENDIX P II: CONNECTION DIAGRAM AND PARAMETERS OF THE FLOW METER
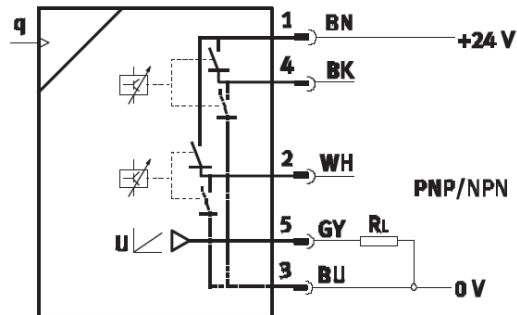
Pin allocation			
Plug M12x1, 5-pin		Pin	Meaning
		1	Operating voltage +24 V DC
		2	Binary output B
		3	0 V
		4	Binary output A
		5	Analogue output C

Flow measuring range[1]) qn as a function of operating pressure p1

Connection Diagram and followed parameter are taken from "Festo Flow sensors SFAM manual".

Siemens SIMATIC ET200SP AI Energy Meter ST Manual [online]. Esslinger am Neckar: Fest, 2014 [cit. 2017-05-15]. Available from: https://www.festo.com/cat/de_de/data/doc_engb/PDF/EN/SFAM_EN.PDF

APPENDIX P III: TABLE WITH A SAMPLE OF USED TAGS

Name	DataType	Default value
rTotalEnergyActual	Real	0
rTotalEnergyMin	Real	0
rTotalEnergyHour	Real	0
rTotalEnergyDay	Real	0
rTotalEnergyMonth	Real	0
rTotalEnergyYear	Real	0
rTotalEnergyDecade	Real	0
rTotalPriceActual	Real	0
rTotalPriceMin	Real	0
rTotalPriceHour	Real	0
rTotalPriceDay	Real	0
rTotalPriceMonth	Real	0
rTotalPriceYear	Real	0
rTotalPriceDecade	Real	0
fbCalculateTotalEnergy_Instance	fbCalculateTotalEnergy	
fbCalculateTotalPrice_Instance	fbCalculateTotalPrice	

Rests of the tags are in "PLC and HMI tags" xlsx file which is attached to this thesis.